Title

Peripheral Neuropathy in Mouse Models of Diabetes

Journal

Current Protocols in Mouse Biology, 6(3)

ISSN

2161-2617

Authors

Jolivalt, Corinne G
Frizzi, Katie E
Guernsey, Lucie
et al.

Publication Date

2016-09-01

DOI

10.1002/cpmo.11

Peer reviewed

HHS Public Access

Author manuscript

Curr Protoc Mouse Biol. Author manuscript; available in PMC 2017 September 01.

Published in final edited form as:

Curr Protoc Mouse Biol. ; 6(3): 223–255. doi:10.1002/cpmo.11.

PHENOTYPING PERIPHERAL NEUROPATHY IN MOUSE MODELS OF DIABETES

Corinne G. Jolivalt, **Katie E. Frizzi**, **Lucie Guernsey**, **Alex Marquez**, **Joseline Ochoa**, **Maria Rodriguez**, and **Nigel A. Calcutt**

Department of Pathology, University of California San Diego, La Jolla, CA 92093

Abstract

Peripheral neuropathy is a frequent complication of chronic diabetes that most commonly presents as a distal degenerative polyneuropathy with sensory loss. Around 20–30% of such patients may also experience neuropathic pain. The underlying pathogenic mechanisms are uncertain and therapeutic options are limited. Rodent models of diabetes have been used for more than 40 years to study neuropathy and evaluate potential therapies. For much of this period, streptozotocin-diabetic rats were the model of choice. The emergence of new technologies that allow relatively cheap and routine manipulations of the mouse genome has prompted increased use of mouse models of diabetes to study neuropathy. In this article, we describe the commonly used mouse models of type 1 and type 2 diabetes and provide protocols to phenotype the structural, functional and behavioral indices of peripheral neuropathy with a particular emphasis on assays pertinent to the human condition.

Keywords

Peripheral neuropathy; Allodynia; Hyperalgesia; Hypoalgesia; Nerve conduction velocity; Nerve morphometry; Skin biopsy; Corneal confocal microscopy; Type 1 diabetes; Type 2 diabetes

4. INTRODUCTION

The value of any animal model of disease lies with its fidelity to the human condition. When considering use of animal models of human disease, two questions should be initially asked: does the animal have the appropriate features of the disease and, if so, does this feature arise by the same process? Few animal models are faithful replicates of human disease and discrepancies can sometimes be reasonably mitigated by other advantages such as ability to perform experiments not permissible or practical in humans, accelerated disease progression that makes longitudinal studies viable or reduced cost compared to clinical research. This balance between ability to perform studies and their clinical pertinence should also be frequently re-assessed when designing experiments that seek to identify pathogenic mechanisms or assess efficacy of therapeutic interventions.

Corresponding author: Nigel A. Calcutt, Phone: 1 858 534 5331, Fax: 1 858 534 1886, ncalcutt@ucsd.edu.

Conflict of Interest

The authors have declared no conflicts of interest for this article.

John Steinbeck is frequently misquoted to make the case that experimental studies in mice may offer useful insights into diseases of man. Diabetic mice do show some functional and structural features of neuropathy that resemble those measured in patients, such as slowing of large fiber conduction velocity and depletion of small sensory fibers in the skin and cornea (Beiswenger et al., 2008a; Chen et al., 2013; Quattrini et al., 2007). Other manifestations of neuropathy, including aspects of painful neuropathy such as allodynia (pain to a non-painful stimulus) and hyperalgesia (exaggerated pain to a painful stimulus), have been inferred from behavioral studies that measure stimulus-evoked aversive responses (Lee-Kubli et al., 2014).

Unfortunately, the segmental demyelination, Wallerian degeneration and frustrated regeneration that are the major pathological features of advanced diabetic neuropathy are rarely identified in well prepared material from diabetic rodents – even after half a life span or more of exposure to levels of hyperglycemia that would produce coma and death in humans (Kennedy and Zochodne, 2005). This absence of overt pathology may reflect inescapable features of rodent physiology and anatomy such as short life span (in human years) that limits exposure time to pathogenic mechanisms or physical size that limits absolute axon length. Diabetic mice may therefore be most cautiously viewed as modeling early stages of nerve dysfunction and axonopathy. This phenotype can be presented as a boon, as molecular and biochemical changes in nerve can be investigated with the optimistic interpretation that they precede, predict and perhaps even cause, overt neuropathy. Unfortunately, it also restricts any guarantees of the translation of therapies developed using these models to the overt degenerative neuropathy of the human condition.

This review describes commonly used mouse models of diabetes and describes how to induce type 1 diabetes using the pancreatic β cell toxin streptozotocin (Basic Protocol 1). The assays selected to phenotype neuropathy represent those that illustrate functional disorders common to diabetic mice and humans and their structural counterparts. Large fiber neuropathy is evaluated by measuring nerve conduction velocity (NCV: Basic Protocol 2), paw withdrawal threshold (PWT) to light touch (Basic Protocol 3), and fiber dimensions by light microscopy (Basic Protocol 4), while small fiber neuropathy is evaluated by paw withdrawal to escalating heat (Basic Protocol 5) and the density of small sensory fibers in paw skin (Basic Protocol 6) and the cornea (Basic Protocol 7) by microscopy. A detailed description of the rationale for the choice of these particular assays has been presented in a recently published consensus statement on the phenotyping of peripheral neuropathy in diabetic rodents issued by the Neurodiab Study group of the European Association for the Study of Diabetes (Biessels et al., 2014). Some of the assays used to phenotype diabetic neuropathy are commonly used in other disease models and have been described elsewhere in this series. In such cases we have focused on highlighting modifications specific for diabetic mice.

NOTE: All protocols using live animals must first be reviewed and approved by an Institutional Animal Care and Use Committee (IACUC) or must conform to governmental regulations regarding the care and use of laboratory animals.

5. STRATEGIC PLANNING: CHOOSING A MODEL SYSTEM

5.1: What Type of Diabetes?

Neuropathy occurs in patient with type 1 (insulin deficient) and type 2 (insulin resistant) diabetes. Suggestions that the natural history and presentation of neuropathy may vary between the two types of diabetes are not easy to confirm, given the highly variable natural history and presentation of neuropathy within each type of diabetes. While insulin deficiency accounts for 5–10% of the human diabetic population, most preclinical research to date has been performed in rodent models of type 1 diabetes. However, as data accumulates in other models of diabetes, it is becoming apparent that mouse models of both type 1 and type 2 diabetes develop broadly similar manifestations of diabetic neuropathy, such as large nerve fiber conduction slowing, progressive loss of thermal sensation and depletion of epidermal fibers. Differences in the time of onset and rate of progression of these features may occur between diabetes types, within one type of diabetes depending on mouse strain and within any given cohort of mice of the same strain and diabetes type, depending of severity of disease. Choice of mouse model of diabetes may be influenced by perceived clinical relevance (type 2 diabetes represents 90–95% of all clinical cases), the primary pathogenic mechanism (insulinopenia vs insulin resistance and hyperinsulinemia), viability for particular assays (extreme obesity in type 2 diabetic mice can impede performance in some behavioral tests independent of neuropathy), or cost.

5.2: What Model of Type 1 Diabetes?

Type 1 diabetes in humans is caused by autoimmune damage to pancreatic β cells, with subsequent insulinopenia and hyperglycemia. The dominant focus on hyperglycemia as a primary cause of clinical and experimental diabetic neuropathy (Tomlinson and Gardiner, 2008) has more recently been complemented by recognition that deficiency of insulin and C-peptide, in their capacity as neurotrophic-like factors, may also have a distinct pathogenic role (Wahren and Larsson, 2015; Xu et al., 2004). How insulinopenia and hyperglycemia are generated in specific models of type 1 diabetes has, historically, not been a particularly pertinent consideration when investigating mechanisms underlying neuropathy.

Streptozotocin—Early use of alloxan to damage pancreatic β cells has largely been superseded by streptozotocin, an antibiotic product of Streptomyces *achromogenes*. Streptozotocin, commonly abbreviated to STZ and occasional written as streptozocin, is easier than alloxan to dose titrate so that it induces insulin (and C peptide) deficient hyperglycemia without acute cachexia and death (Mansford and Opie, 1968). The STZ-diabetic mouse model is inexpensive and widely used but is also the most fraught with potential variability. There can be considerable inter-batch variability in potency of STZ, so that the severity of induced diabetes can vary markedly both between and within laboratories. This variability can affect the number of mice that become diabetic in a cohort of STZ injected animals (conversion rate), the severity of insulinopenia, the onset and magnitude of indices of neuropathy and the duration of animal survival. It is therefore particularly important to design experiments to include all groups necessary to form a complete and interpretable study, as it can be problematic to make between-study comparisons, even within the same laboratory.

Genetic models—There are mouse models of type 1 diabetes that exhibit either genetically driven autoimmune damage to the pancreas (NOD mouse) or misfolding of pro-insulin leading to reduced insulin secretion and pancreatic β cell failure ($Ins2^{Akita}$ mutation on assorted backgrounds). These mice are commercially available and described in detail elsewhere in the Current Protocols in Mouse Biology series (Leiter and Schile, 2013). They have not been widely used in neuropathy studies to date, presumably due to limited availability and relatively high cost. Where studied, the neuropathy phenotype of these genetic models resembles that of STZ-diabetic mice, supporting the argument that neuropathy is not caused by STZ-induced direct neurotoxicity. The advantage gained from studying pathogenic mechanisms of diabetic neuropathy in genetic models of diabetes is uncertain. Indeed, NOD mice are generally avoided in neuropathy research due to the potential for direct damage to nerves by the immune system (Bour-Jordan et al., 2013).

5.3: What Model of Type 2 Diabetes?

Metabolic syndrome and type 2 diabetes initially arise in humans due to impaired insulin receptor function, prompting hyperinsulinemia and concurrent hyperglycemia. In time, pancreatic β cells may fail so that there is insulinopenia and late stages of disease resemble type 1 diabetes. There are a number of inbred mouse strains that develop insulin resistance, hyperinsulinemia and, in some cases, hyperglycemia. These include the db/db mouse (primary leptin deficiency that leads to polyphagia), the ob/ob mouse (leptin receptor dysfunction) and mice with insulin receptor knock down. Normal mice provided with a high fat diet are also used. A detailed description of the general physiology of rodent models of obesity, metabolic syndrome and type 2 diabetes is provided elsewhere in the Current Protocols in Mouse Biology series (Lutz and Woods, 2012).

Some of the earliest detailed descriptions of functional and structural indices of peripheral neuropathy in diabetic rodents were made using the db/db mouse model of type 2 diabetes. Mice fell out of favor as models of diabetic neuropathy due to the assumption that they lacked polyol pathway activity in nerve. This was disproven (Calcutt et al., 1988) and the dramatic rise in obesity-related diseases has accelerated use of rodent models of type 2 diabetes in attempts to most faithfully model the systemic phenotype accompanying neuropathy. The peripheral neuropathy phenotype of models of metabolic syndrome and type 2 diabetes is not markedly different from that of type 1 diabetic mice (Guilford et al., 2011), although neuropathy is most dramatic in db/db mice once they have progressed to insulinopenia after around 6 months of age. One interesting exception is the Swiss Webster mouse fed a 60% fat diet. These mice develop neither obesity nor peripheral neuropathy over a time span (6 months) where both obesity and neuropathy are clear in C57Bl/6J mice fed the same high fat diet (Anderson et al., 2014).

The similarity of neuropathy phenoypes between models of type 1 and type 2 diabetes and within specific models of each form of the disease may have implications for pathogenic mechanisms. However, while it has been broadly assumed that this supports hyperglycemia as the dominant primary pathogenic mechanism, it should also be noted that peripheral nerves express functional insulin receptors and in some models of type 2 diabetes develop

insulin resistance (Grote et al., 2013), so that impaired insulin signaling may also be common to both type 1 and type 2 diabetes.

NOTE: All protocols using live animals must first be reviewed and approved by an Institutional Animal Care and Use Committee (IACUC) or must conform to governmental regulations regarding the care and use of laboratory animals.

6. BASIC PROTOCOLS

BASIC PROTOCOL #1: Induction of diabetes using STZ

STZ dose: Many laboratories have developed their own preferred regime, ranging from single high doses to lower doses given repeatedly over many days. In our experience, a single dose of 180–200 mg/kg can cause death of 10–50% of a cohort within 1 week of injection and the remaining mice will show marked insulinopenia, weight loss and die within 12 weeks if not given exogenous insulin. This is particularly true for inbred strains, whereas outbred Swiss Webster mice are more resilient. At the other end of the dosing range, we find that using multiple low (40–60 mg/kg) doses of STZ across 5 days, which was designed to prevent acute STZ-induced nephrotoxicity (Breyer et al., 2005), produces a milder insulinopenia in which mice may not develop indices of neuropathy, such as NCV slowing, for 8–12 weeks despite marked hyperglycemia (Calcutt, unpublished observations). Our current preference is to give 90 mg/kg STZ on two consecutive days for adult (20–25g) inbred mice and 100 mg/kg on two consecutive days for adult (25g+) outbred mice. This regime produces few initial deaths, 90% or greater conversion rates and minimal weight loss in mice that survive untreated for 3–6 months without cohort depletion (see Table 1).

Materials

Mice

Streptozotocin (Sigma-Aldrich Cat #: S0130-5G)

0.9% sterile saline

25 gauge needle

Glass scintillation vials or similar

Glucose meter and strips (Lifescan, One Touch Ultra system or similar).

Procedure

1. Fast mice overnight *(STZ uptake into pancreatic β cells is achieved via the GLUT-2 glucose transporter and a reduction in circulating glucose during fasting allows increased STZ uptake and a greater likelihood of success at inducing diabetes)*.
2. Prepare STZ
   a. The dose of STZ depends on mouse weight:
      i. <18 g – wait for weight gain

ii. 18–20 g – STZ @ 100 mg/kg

iii. 20–25 g – STZ @ 90 mg/kg

iv. >25 g – STZ @ 85 mg/kg

b. Pre-weigh streptozotocin in batches that are enough to dose 5–6 animals. *For 10 mice in the 18–20g range, prepare 2 × 10mg batches of STZ in glass vials*.

3. Add sterile saline to the STZ to give a 10 mg/ml solution and shake to dissolve until a clear, straw colored solution is achieved. *Add 1.0 ml saline to 10mg STZ*.

4. Administer STZ solution via intraperitoneal injection at 10ml/kg. *Each 20g mouse will receive 200μl of STZ solution*.

5. Work quickly and efficiently through all mice to be injected from the STZ solution. *STZ in saline has an effective life of about 5 minutes and thereafter diabetogenic activity will decline and mice will not develop overt hyperglycemia*.

6. Wait 1 hour and then return food to cages for the rest of the day.

7. Fast mice overnight.

8. Repeat steps 2–6.

9. Five days after the second STZ injection collect a drop of blood via 25 gauge needle prick to tail and measure blood glucose concentration using a test strip and glucose meter.

   a. Mice are considered diabetic when blood glucose is at least 15 mmol/L (270 mg/dl)

   b. If the glucose value is ≤ 15 mmol/L, steps 1–8 can be repeated one week later, if approved by the local IACUC.

BASIC PROTOCOL #2: Measurement of nerve conduction velocity

Large fiber neuropathy can be detected by electrophysiology (nerve conduction velocity), evoked behavior (responses to light touch) and histology (nerve trunk morphometry). Slowing of large fiber NCV is the current gold standard for determining neuropathy in diabetic patients and for assessing efficacy of potential therapeutics. Motor and sensory NCV slowing is also an early feature of diabetes mice with type 1 or type 2 diabetes and may be detected within weeks of onset of diabetes.

Materials

PowerLab 4/30 and pre-amplifier (AD Instruments)

Computer running LabChart Pro Software (AD Instruments)

Temperature controller set to 37±0.5°C, with fine wire thermistor probe (Yellow Springs Instruments model 73ATC)

Mobile heat lamp connected to the temperature regulator

Four platinum-tipped sub-dermal needle electrodes (Grass Technologies, Cat #: F-E2)

EZ anesthesia Versaflex small animals anesthesia system consisting of a water circulating heating pad, anesthesia induction chamber, isoflurane regulator and delivery system (Braintree Scientific Inc. Cat #: EZ-7150).

Isoflurane

Oxygen

Sterile surgical instruments and povidone-iodine (Betadine)

Procedure

1. Place the mouse in an induction chamber and anesthetize using 2.5–4ppm isoflurane/oxygen.
2. Remove mouse when lightly anesthetized and transfer to the circulating water heated pat, with anesthesia maintained via a facemask connected to the isoflurane regulator.
3. To ensure stable nerve temperature:
    a. Shave the hair from the hind limb using a scalpel blade.
    b. Expose the sciatic nerve by separating the skin and muscle covering the femur.
    c. Place the wire thermistor tip adjacent to the sciatic nerve, close the incision with a surgical clamp and monitor local temperature.
    d. Place lab tissue or another protective covering over the head and tail of the mouse to protect them from unnecessary heat.
    e. Warm the hind limb using the heating lamp until the nerve temperature stabilizes at 37°C. The temperature controller will turn off the heating lamp when temperature rises above 37°C and turn it back on when temperature falls below 37°C. *Note: Be patient and do not move the heating lamp too close to the mouse, as this can burn the ears and tail.*
4. Insert two recording electrodes into the interosseous muscles between the animal's second, third and fourth toes and secure the foot to the heating pad with lab tape
5. Place a subcutaneous grounding electrode into the neck.

6. Set the PowerLab stimulator to deliver a 200mV, 50 μs duration square wave stimulus every 2 seconds.
7. Insert the stimulating electrode into the ankle near the Achilles tendon.
8. Adjust the simulation intensity until the resulting M and H waves are clear and maximal (Figure 1).
9. Remove the electrode and insert it into the sciatic notch at the hip.
10. Record the resulting M and H waves.
11. Repeat this process three times, switching between the ankle and hip locations accordingly.
12. Stretch the leg and measure the distance between the stimulation sites at the hip and ankle.
13. The animal can now be removed from the general anesthesia
14. Close the incision and clean with betadine.
15. Observe the mouse until it recovers then return to its home cage.
16. The first pair of peaks (M waves) represents the stimulation of motor nerves at the ankle (1st peak) and hip (2nd peak) (Figure 1).
17. The second pair of peaks (H waves) represents the stimulation of the sensory nerves (H wave) at the hip (1st peak) and ankle (2nd peak)
    a. The H wave amplitude is sensitive to depth of anesthesia and H waves may not be readily apparent in mice, as the relatively small body size makes maintaining an appropriate and consistent level of anesthesia difficult.
    b. If sensory nerve testing is the primary objective, an injectable anesthetic is a preferable alternative to inhaled isoflurane.
18. To calculate NCV (in m/s):
    a. Choose the most consistent peaks and record their maximum or minimum values.
    b. Determine the difference in time between each pair of peaks.
    c. To correct for outliers and electrode placement errors, use the median latency of the three pairs of recordings.
    d. Divide this value by the length of the sciatic nerve.

BASIC PROTOCOL #3: Measuring tactile allodynia in diabetic mice

Behavioral responses to light touch are independent of capsaicin-sensitive small sensory fibers (Khan et al., 2002) and likely incorporate function of large myelinated sensory fibers

that terminate in the dermis. Diabetic rodents develop increased sensitivity to a series manual von Frey filaments within 2–4 weeks of induction of diabetes (Calcutt et al., 1996). A similar increase in sensitivity can be detected using electronic von Frey filaments, although we suspect that the two approaches measure different parameters as the time course to peak efficacy of the anti-pain drug gabapentin is not identical when using manual and electronic filaments (Lee-Kubli et al., 2014). The method originally validated by Chaplan and colleagues (Chaplan et al., 1994) and its variants have been described elsewhere in the Current Protocols in Mouse Biology Series as Basic Protocol 6 (Minett et al., 2011). For diabetic mice we use the following modifications:

Materials

Calibrated von Frey filaments (Kom Kare Inc)

Electronic von Frey anesthesiometer (IITC Life Sciences Inc.)

Testing stand with 2 mm^2 mesh surface (self constructed)

Glass 250ml beakers to act as restraint chambers

Procedure

1. Place mice on the testing stand within the restraint chamber and allow to acclimate for 15 minutes or until exploratory behavior has ceased. *We have constant "white noise" in the testing room to mask any sudden noises that can startle animals.*
2. The sequence of manual von Frey filaments used is: 2.44, 2.83 3.22, 3.61, **3.84**, 4.08, 4.31, 4.56, 4.74 with the 3.84 filament being used as the starting filament.
3. Apply enough pressure to the filament to cause buckling for 1 sec and repeat the application 5 times, making sure that the filament never leaves the plantar surface of the hind paw unless the mouse responds.
4. When using the electronic von Frey filament, apply the tip of the device to the plantar surface and gradually increase applied force until the mouse withdraws from the filament tip, at which point the maximum applied force is displayed.
4. Do not test while a mouse is urinating, rearing or grooming.
5. Do not leave diabetic mice in their testing chambers for more than an hour, as they may become dehydrated and will stop responding to stimuli.

BASIC PROTOCOL #4: Morphometry of myelinated fibers in nerve trunks

A cross section of sciatic nerve, processed to resin blocks and cut into 0.5–1.3 μm thick sections for viewing by light microscopy will allow visualization and measurement of large motor and sensory nerve fibers, along with blood vessels and cells of the perineurium. Distal branches of the sciatic nerve, the saphenous nerve or the sensory or motor nerve roots may be used to focus on either large motor or sensory nerve fibers. Great care must be taken at all stages, as dissection and fixation artifacts, or indeed normal features of fibers when

sectioned at certain points along their length, can be mistaken for myelin or axonal pathology.

Materials

Equipment

Dissection tools, including fine forceps

Matchstick or wooden applicator

20 ml scintillation vials (Fisher, catalog #7450520)

Tissue rotator (EMS, catalog #71780-10)

Vacuum desiccator

PELCO 105 flat embedding molds (Ted Pella, catalog #105)

10 mL plastic syringe

Oven at 60°C

Resin block holder

Dissecting microscope

Single edge blades (WecPrep, EMS catalog #71933-50)

Glass strips (Leica catalog #16840031) and knife maker (Leica model EM KMR2)

Glass knife boats (EMS, catalog #71008)

Ultramicrotome (Sorvall, MT-1)

Solutions and Reagents (see Section 10 for recipes)

2.5% glutaraldehyde

0.1M sodium phosphate buffer

Ethanol (100% and assorted dilutions)

2% aqueous osmium tetroxide (EMS, catalog #19152)

Propylene oxide (EMS, catalog #20411)

DDSA (EMS, catalog #13701)

Araldite 502 resin (EMS, catalog #10900)

Embed 812 (EMS, catalog #14901)

DMP-30 (EMS, catalog #13600)

p-Phenylenediamine (Sigma, catalog #P6001)

CytoSeal 60 mounting medium (Thermo Fisher, catalog #8310-4)

Procedure—Day 1 (primary fixation):

1. We generally use immersion fixation, as detailed below, as it allows other tissues to be collected for biochemical analyses. We find no notable differences in nerve morphology or morphometry when comparing nerves fixed by perfusion or immersion, although the former may preserve circularity of endoneurial blood vessels (Schenone and Dyck, 1987).

2. Kill mouse by an IACUC-approved method then expose and transect a 0.5–1.0 cm segment of peripheral nerve without stretching or otherwise compromising its structural integrity. Use forceps to grip one of the cut ends of the nerve, lift the nerve gently from the animal, place lengthwise on a stick of wood (applicator or matchstick) to stop the nerve folding and immerse in a scintillation vial containing cold 2.5% glutaraldehyde. The volume of fixative should be ~20 times the volume of the tissue.

3. Place the vial containing fixative and tissue in a refrigerator at 4°C and store overnight (18–30 hrs).

Day 2 (secondary fixation):

4. Pour off fixative (see below for safety procedures), wash nerve with 20 ml 0.1M sodium phosphate buffer, pour off buffer, repeat the wash and then remove the nerve and gently remove any unwanted fat and muscle using fine forceps and a blade to ensure evenly distributed penetration of osmium.

5. Measure the cross sectional diameter of your nerve to estimate osmication time. Osmium penetrates tissue from all sides at roughly 0.5 mm/hour, so a mouse nerve with a diameter of 1 mm should osmicate for 1 hour.

6. Drain the 0.1M sodium phosphate buffer then add sufficient 2% osmium to cover the tissue in the vial (3–4 ml). Cap the vial and place on the rotator for the predetermined amount of time.

7. Rinse in 5–10 ml distilled water, drain and repeat the rinse.

8. Immerse in 20 ml 0.1M sodium phosphate buffer and refrigerate until ready to dehydrate and embed (minimally overnight, maximally up to 2 months).

Day 3:

9. Remove the buffer and rinse the nerve twice in 5–10 ml distilled water.

10. Dehydrate the nerve by taking it through the following steps. For each step, fill the vial with enough solution to cover the tissue, cap the vial and then place the vial on the rotator for the time specified:

    a. 30% ethanol (EtOH) rinse followed by 30% EtOH wash: 10 min

    b. 50% EtOH rinse followed by 50% EtOH wash: 10 min

    c. 70% EtOH rinse followed by 70% EtOH wash: 10 min

    d. 95% EtOH wash: 15 min × 2

e. 100% EtOH wash: 15 min × 2

f. Propylene oxide: 15 min × 2.

11 Incubate in a 50%-50% mixture (see Section 10: Reagents and Solutions) of resin and propylene oxide for 2 hours, with each vial covered and placed on a rotator.

12 Incubate in 100% resin for 30 min, with each vial covered and placed on a rotator.

13 Place uncapped vials containing tissue and also the remainder of the 100% resin into a vacuum desiccator overnight. This will remove air bubbles from the resin and help to fully infiltrate the tissue.

Day 4 (embedding):

14 Print or handwrite labels for each block and put paper labels in each well of the embedding mold. Do not use pen ink, as it fades in the resin.

15 Using a 10 ml syringe, slowly add 100% resin to each mold from the extra resin that was vacuum dried overnight. Try to minimize the amount of bubbles created.

16 Place one nerve in each well and orientate so that it is as flat and straight as possible with one cross sectional edge touching the cutting surface (the trapezoidal end of the mold).

17 Gently add 100% resin to completely fill the well as it will decrease in volume as it polymerizes. Remove any air bubbles by puncturing them or moving them to the non-trapezoidal end of each mold with a straightened paperclip or forceps, then re-adjust nerve orientation as needed.

18 Place molds in a 60°C oven overnight (12–18 hrs). When they have hardened, remove them from the oven and allow to cool at room temperature before removing the blocks from the molds.

Day 5 (sectioning):

19 Mount a resin block in a block holder with the trapezoidal end facing up.

20 Using a dissecting scope and single-edged razor blade, trim away the excess resin at a 45 degree slope from around the top 1–2 mm of the nerve sample. The face of the block should remain in a trapezoidal shape, but should mainly consist of nerve with a small amount of surrounding resin.

21 With a new blade, gently trim the face of the block to expose the surface of the tissue. Remove the block from the block holder.

22 Break glass strips into glass knives using glass knife maker. *Where possible, use knives on the day they were made, though they may still be sharp the following day.*

23 Attach knife boats to the glass knives with hot wax or nail polish. Allow to dry.

24 Secure the trimmed block and the prepared glass knife into the appropriate areas on the ultra-microtome. Fill the knife boat with distilled water that has passed through a 0.22 μm filter.

25 Section the block to between 0.5 μm (semi-thin) to 1.3 μm (thick). Thickness of the section can be evaluated by its interference color (0.5 μm = pink-bluish, 1 μm = blue-green with pink hints, 1.3 μm = green) as it floats on the water-filled knife trough.

26 Collect the sections into a droplet of filtered distilled water on an uncoated glass slide using a glass rod.

27 Place the slide on a preheated hot plate – the droplet of water should evaporate within 3 minutes.

Staining with *p*-Phenylenediamine (PPD):

28 Prepare 2% PPD stain in 50% ethanol and stir for 3 hours. Store at room temperature in an amber glass bottle covered in aluminum foil. Let stain sit for 5 or more days before use.

29 Filter PPD stain through a 0.22 μm nylon filter.

30 Immerse slides in PPD in a staining jar and cover the jar to prevent evaporation.

31 Stain for 20 minutes at room temperature. Stain intensity can be checked using a light microscope.

32 Drain stain out of staining jar. Stain can be reused.

33 Gently rinse slides twice with tap water (enough to cover slides completely).

34 Gently rinse slides twice with deionized water (enough to cover slides completely).

35 Gently rinse slides twice with distilled water (enough to cover slides completely).

36 Place slides in a slide rack and dry the slides in a 60°C oven for 15–30 minutes.

37 Remove slides from the oven and cool to room temperature.

38 Mount using a non-aqueous mounting medium (CytoSeal 60).

Nerve Analysis and Quantification:

39 Select a single section on each slide that is well stained and free from artifact, such as folds, tears, and knife marks. Mark the section for future reference.

40 View section under a light microscope, capture images and transfer to an image analysis program of your choice.

41 Parameters such as axon diameter and area and myelinated fiber diameter and area are measured, and derived values such myelin thickness and area and fiber g-ratio calculated, only if:

- **a.** There is adequate fixation across the the nerve cross section, as indicated by even and well-contrasted staining (Figure 2A)
- **b.** There is no evidence of mechanical artifact, as caused by stretching, crushing or distorting the nerve during processing, in the cross section (Figure 2A and 2B).
- **c.** Both the axon and its myelin sheath of each fiber to be counted have a circular or oval shape and the myelin sheath is intact (Figure 2A and 2C)
- **d.** The fiber cross-section is not paranodal (Figure 2C)
- **e.** The cross-section does not include Schmidt-Lanterman incisures (Figure 2C)
- **f.** The cross-section does not include a Schwann-cell nucleus (Figure 2C)

Safety

1. All reagents should be treated as hazardous waste so please consult with your local safety authorities before starting to clarify use and disposal procedures.
2. Osmium tetroxide is extremely toxic. Use caution, work in the hood, and wear double nitrile gloves. If a spill is suspected, you should neutralize the osmium tetroxide by spraying the area with corn oil. If the corn oil turns black there was a spill. Place anything exposed to osmium into the appropriate hazardous waste jar.
3. Resin is highly toxic in liquid form and penetrates nitrile gloves. Change gloves and wash hands if you suspect contact with liquid resin or resin components. Once polymerized and solid, resin is non-toxic. At room temperature it polymerizes in about a month, but at 60°C it will harden in 24 hr so you can place any waste resin or objects that touched resin in the oven overnight.

BASIC PROTOCOL #5: Measuring paw thermal response latency

Small sensory fiber dysfunction may be evaluated by quantification of behavioral responses to heat and has a structural correlate in measuring nerve fiber density in the skin and the cornea. Heat pain is transduced by small sensory C fibers that terminate in the epidermis. Diabetic rats develop an initial paw thermal hyperalgesia that, in the absence of insulin therapy, can progress to hypoalgesia (Calcutt et al., 2004). We find a similar progression in STZ-diabetic mice, although onset of hypoalgesia may occur more quickly (Beiswenger et al., 2008a). We use the protocol described elsewhere in the Current Protocols in Mouse

Biology as Basic Protocol 4 (Minett et al., 2011), with the following modifications for diabetic mice:

Materials

Thermal nociception test device (UARD) as validated elsewhere (Dirig et al., 1997).

Glass 250ml beakers to act as restraint chambers

Procedure

1. Allow the apparatus surface to warm to 30°C.
2. Move the arm to position the heat source immediately below the temperature sensor.
   - **a.** Activate heating and record the temperature every 5 seconds for 20 seconds.
   - **b.** Temperature should increase at approximately 1 degree per second to activate heat sensitive c fibers (Yeomans et al., 1996; Yeomans and Proudfit, 1996). Adjust the heating rate as necessary until 1°C/second is achieved (Figure 3).
   - **c.** We measure a time:temperature curve at least three times during a test day, before onset of the mouse testing, at half way though the testing and at the end of testing.
   - **d.** An average temperature:time curve can be constructed from all calibration curves produced on each testing day.
3. Place mice in their individual testing chambers and allow them to acclimate to their surroundings for at least 15 minutes or until exploratory behavior has ceased. *We use constant "white noise" in the testing room to mask any sudden noises that can startle animals.*
4. Do not measure responses during grooming or urination and clean both the glass surface of the Hargreaves apparatus and the mouse following urination, as a thin layer of urine can alter surface heating rate.
5. Perform measurements exactly as described in the source protocol (Minett et al., 2011).
6. As diabetes is a systemic disease, data can be collected from both hind paws. We generally perform 3 separate response latency measurements on each paw, at 5 minute intervals, take the median of the triplicate to represent each paw and then the mean of the two medians to represent response latency for each animal.
7. This value in seconds is then converted to response temperature using the calibration curve produced for that day (see step 2 and Figure 3).

8. Do not leave diabetic mice in their testing chambers for more than an hour, as they may become dehydrated and will stop responding to stimuli.

BASIC PROTOCOL #6: Epidermal innervation

Loss of small sensory fibers in the epidermis is common to both diabetic patients (Kennedy and Zochodne, 2005) and mice (Beiswenger et al., 2008a). We describe a widely used method for viewing all nerves in the epidermis and dermis using skin samples taken from the plantar surface of the hind paw processed to paraffin blocks and cut as 6μm sections before immunostaining for the pan-neuronal protein, PGP9.5. Hairy skin may also be used, with the caveat that innervation organization and density is quite different around hair follicles and sweat glands. Selective visualization of specific neuronal types may be achieved by using alternative antibodies for immunostaining, such as those directed at substance P.

6.1 Processing to blocks and sectioning

Materials

Equipment

Tissue Processing Embedding Cassette (EMS #70073-A)

Superfrost Plus Slides (Fisherbrand #12-550-15)

Tissue Processor (Leica TP1020)

Embedding Center (Leica EG1160)

Rotary Microtome (Leitz 1512)

Solutions and Reagents

Isoflurane

4% Buffered Paraformaldehyde (*Section 10*)

0.1 M Sodium Phosphate Buffer (*Section 10*)

Ethanol (100% and dilutions: *Section 10*)

Xylene (Fisher #X3S-4)

Paraplast Plus Paraffin (Leica #39602004)

Procedure

1. Kill mouse by an IACUC-approved method and dissect the hind paw plantar skin:
   a. Using a razor blade, make a lateral incision along the right and left sides of the plantar hind paw glabrous skin, getting as close to the hairy skin as possible.
   b. Make another incision between the digits and inter-digital pads, essentially creating an incision triangle from pads to heel.

c. Using dissecting forceps, slightly lift an edge of the skin at the heel and slide a razor blade underneath.

d. Cut the glabrous skin from the underlying plantar fascia and bone.

2. Arrange the plantar skin flat on a piece of plastic that has multiple holes punctured in it to prevent folding during fixation.

   a. Repeatedly puncture a weighing dish or other plastic with a 20 gauge needle to allow free access of fixative to all aspects of the tissue.

   b. Cut the perforated plastic into squares, each just large enough to mount a skin sample.

   c. Place the skin, epidermis up, onto the plastic square.

3. Immersion fix overnight at 4° C in 10× volume of 4% buffered paraformaldehyde.

4. Rinse the tissue 3× by gently agitating in 10–20 ml of 0.1 M sodium phosphate buffer (1:1 distilled water and 0.2 M sodium phosphate buffer.

5. Tissue can be stored in 0.1 M sodium phosphate buffer at 4°C for up to 1 month until processing to paraffin blocks.

6. Using a lead pencil (not ink, which is erased by reagents used in tissue processing), write the sample identification number on an embedding cassette.

7. Use forceps to gently lift the skin sample from the plastic restraint, remove it from buffer and place into the cassette.

8. Store the tissue-filled cassette in 0.1 M sodium phosphate buffer until ready to process into paraffin.

9. Prepare the reagents in your tissue processor at least 12 hours before use, to give the paraffin pellets time to melt:

Stations #1 and 2:	70% ethanol
Stations #3 and 4:	95% ethanol
Stations #5, 6, and 7:	100% ethanol
Stations #8, 9, and 10:	Xylene
Stations #11 and 12:	Paraffin

   NOTE: Reagents should be replaced if they are more than 1 month old or have been used more than 5 times.

10. Place the tissue-filled cassettes (step 8) into the processing basket and lower the basket into the 70% ethanol station.

11. Dehydrate by immersion with gentle agitation and vacuum (if available):

    a 70% ethanol for 5 min

b 70% ethanol for 113 min

c 2 × 95% ethanol for 113 min each

d 3 × 100% ethanol for 113 min each

12. Clear by immersion with gentle agitation and vacuum (if available):

e 3 × xylene for 113 min each

13. Infiltrate by immersion with gentle agitation and vacuum (if available):

f 2 × paraffin for 173 min each

NOTE: Remove the cassettes from the tissue processor within 1 hour of the end of station 12 (paraffin). The infiltrated tissues can remain at room temperature in their cassettes until you are ready to embed into blocks.

14. Turn on embedding center at least 3 hours before use to allow the paraffin to melt. Add fresh paraffin pellets to the paraffin reservoir and cassette bath as needed.

15. Place stainless steel molds into the mold tray to preheat.

16. Verify that the forceps holders have some paraffin in the holes – the molten paraffin will heat forceps better than warm air.

17. When you are ready to begin embedding, place a handful or two of tissue-filled cassettes into the cassette bath and allow the surrounding paraffin to melt.

NOTE: Continue adding a few more cassettes into the bath as you work so they have time to fully melt but don’t soak in the hot paraffin for hours at a time.

18. Working with one cassette at a time, remove the skin from the cassette onto a warmed metal plate. Trimming tissues directly on the embedding center may damage the non-stick coating.

19. Using a warm razor blade, trim a small portion from the ends of the inter-digital pads and the heel to create clean ends to your tissue, then cut in half from pads to heel.

20. Embed both halves of the tissue into the same block with the fresh, longitudinal, cuts touching the bottom of the mold. This cleanly exposes the epidermis, dermis, hypodermis and any underlying tissue for sectioning:

a. Fill a warm mold with molten paraffin until it nearly overflows.

b. Working quickly and using warmed forceps, place the tissue into the mold (keeping in mind that the bottom of the mold will become the face of the final block).

c. Gently move the filled mold onto the refrigeration spot of your embedding center to begin cooling the block. If needed, hold the tissue in place with heated forceps until the bottom of the mold cools and solidifies the tissue in place.

d. Working quickly, place the labeled cassette onto the mold and press down firmly.

e. Working quickly, move the mold/cassette combination back under the paraffin dispenser nozzle and finish filling the mold so that the cassette is filled with paraffin as well.

f. Chill the finished molds until the paraffin fully solidifies and the blocks easily pop out of the molds (5–10 min).

21. The paraffin blocks can be stored at room temperature indefinitely, but beware of storing the blocks near lab hotspots (heater vents, hotplates, freezers, etc.) as the paraffin can melt or become disfigured.

22. Prepare a 40°C water bath next to your rotary microtome.

23. Cut the paraffin block at 6μm, discarding initial sections until the entire length of the biopsy is present within the section. Blocks are easier to section if there are chilled in the refrigerator prior to cutting and sectioned while still cold.

24. Carefully cut a ribbon of 6μm sections and expand them by floating in the water bath.

25. Select a few of the best-looking sections and mount them on microscope slides.

26. Evaluate the sections at 40× magnification to ensure that the epidermis and dermis are included in the entire section of the tissue.

27. Dry the slides overnight at room temperature in a dust-free environment before staining.

6.2 Immunohistochemistry against protein gene product 9.5

Materials

Equipment

Hydrophobic Marker (5 mm PAP Pen, Sigma, #Z377821)

Slide Humidifier (StainTray, Simport Plastics, #M920-1)

Solutions and Reagents

Xylene (Fisher #X3S-4)

50%, 70%, 95%, and 100% Ethanol (Section 10)

3% Hydrogen Peroxide in distilled water

1× Phosphate Buffered Saline (Section 10)

Vectastain ABC Kit, Rabbit IgG, Vector Laboratories, #PK-4001 (includes normal goat serum, 2° antibody, and avidin/biotin complex)

anti-Protein Gene Product 9.5, Rabbit anti-Human, Polyclonal IgG (AbD Serotec, #7863-0504)

NovaRed Substrate Chromagen Kit (Vector Laboratories, #SK-4800)

Gill's Hematoxylin (Vector Laboratories, #H-3401)

Toluene-based Mounting Medium (Cytoseal 60, Thermo Scientific, #8310-4)

Procedure

28 Label the slides using a pencil (not ink or markers that can be removed by xylene).

29 Dry the 6 μm-thick paraffin sections of skin biopsies fully by incubating the slides in an oven at 60° C for 1 hour. Allow the slides to come to room temperature for at least 3 min.

30 Clear the sections by immersing the slides in xylene 3 times for 3 min each.

31 Rehydrate the sections by immersing the slides in enough of each the following reagents to fully cover the slides:

- **a** 100% ethanol, 2 times for 3 min each
- **b** 95% ethanol, 2 times, for 3 min each
- **c** 70% ethanol, for 3 min
- **d** 50% ethanol, for 3 min
- **e** distilled water, for 3 min

32 Quench endogenous peroxidase by immersing the slides in 3% hydrogen peroxide for 15 minutes.

33 Rinse the slides by immersing them in distilled water 3 times for 3 min each.

34 Rinse the slides by immersing them in 1× phosphate buffered saline (section 10) for 3 min.

35 Circle the sections on the slides with a hydrophobic marker.

36 Using the ABC kit, prepare diluted normal goat serum (for about 20 slides): 10 mL 1× PBS + 3 drops normal goat serum.

37 Block nonspecific staining by covering the sections with ~ 500 μl of the prepared normal goat serum and incubating for 30 min in a slide humidifier at room temperature.

38 Prepare a 1:1000 dilution of anti-PGP9.5 antibody solution (for about 20 slides): 5 mL 1× PBS + 5 µL anti-PGP9.5 antibody + 1 drop normal goat serum (from ABC kit).

39 Drain off the goat serum from all the sections, except the negative control.

40 Apply the anti-PGP9.5 antibody solution to all the sections except the negative control and incubate overnight in a humidifier at 4° C.

41 Rinse all of the slides by gently pipetting 1–3 ml of 1× PBS over the sections 3 times, then by immersing the slides in 1× PBS 3 times for 3 min each.

42 Using the ABC kit, prepare the 2° antibody solution (for about 20 slides): 10 mL 1× PBS + 1 drop 2° antibody + 1 drop normal goat serum.

43 Apply ~500 µl of the 2° antibody to each section and incubate for 1 hr in a humidifier at room temperature.

44 Using the ABC kit, prepare the avidin/biotin complex (ABC) solution 30 min prior to use (for about 20 slides): 10 mL 1× PBS + 2 drops of bottle A + 2 drops of bottle B

45 Rinse the slides by gently pipetting 1× PBS over the sections 3 times, then by immersing the slides in 1× PBS 3 times for 3 min each.

46 Apply ~ 500 µl of the ABC solution to each section and incubate for 1 h in a humidifier at room temperature.

47 Rinse the slides by immersing them in 1× PBS 2 times for 3 min each.

48 Rinse the slides by immersing them in distilled water 2 times for 3 min each.

49 Using the NovaRed Chromagen kit, prepare the chromagen solution immediately before use (for about 20 slides): 10 mL distilled water + 6 drops of bottle 1 + 4 drops of bottle 2 + 4 drops of bottle 3 + 4 drops of hydrogen peroxide solution.

50 Apply ~ 500 µl of the chromagen solution to each section and incubate at room temperature for 1 to 5 minutes, or until desired level of red stain appears in each section.

NOTE: The epidermis usually has high background staining, so it is best to rinse the slides as soon as the red stain is visible with the naked eye.

51 Rinse the slides by gently pipetting distilled water over the sections 3 times, then by immersing them in distilled water 3 times for 3 min each.

52 Counterstain the sections by immersing the slides in 10% Gill's Hematoxylin in distilled water for 1 min, or until desired level of stain is achieved.

NOTE: 10% Gill's Hematoxylin can be re-used many times. Store at room temperature in an amber bottle.

NOTE: When freshly made, 1 min of incubation in the counterstain is a reasonable amount of time. If the stain is old or has been re-used many times,

the incubation time should be increased by a few minutes. If the incubation time necessary for good staining exceeds 5 min then it is time to make a fresh solution.

53 Rinse the slides in distilled water until the water runs clear.

54 Dehydrate the sections by immersing the slides in the following reagents:

- **f** 50% ethanol, 3 min
- **g** 95% ethanol, 3 min
- **h** 100% ethanol, 2 times, 3 min each

55 Clear the sections by immersing the slides in xylene 3 times for 3 min each.

56 Mount the slides using a non-aqueous mounting medium, e.g. Cytoseal 60.

57 Allow the slides to dry flat overnight, then store them covered at room temperature indefinitely.

6.3 Quantifying nerve fibers in skin

Materials

Light microscope with digital camera and output to a computer running imaging software (Scion Image freeware or similar).

Removable multipurpose stickers

Lab marker

Notebook

Procedure

58 Look at each sample under a light microscope and pick the best sections.

- **a.** Best sections will have an even and consistent stain, few if any hair follicles, consistent thickness in the epidermis, and a lack of artifacts or tissue folds.

59 Circle each best section with a lab marker.

60 Cover the white label area of the slides with multipurpose stickers to code the tissue.

61 Label the slides with new, random numbers or letters. Keep track of the coding in a notebook.

62 View the tissue and make a crude sketch it in your notebook, highlighting large identifiable structures.

- **a.** Mark the counting starting point, any skipped areas, and other notable details.
- **b.** These notes will be used to accurately measure the skin length.

63 Using the 40X lens, start at one end of the sample and count the Sub-Epidermal Nerve Plexi (SNP) and the Intra-Epidermal Nerve Profiles (IENF) in separate passes (Figure 4).

- **a.** SNP identification:
  - **i.** Only count profiles located in the papillary dermis.
  - **ii.** While counting SNPs, frequently adjust the fine focus of the microscope to help determine if the profile consists of one or more fibers.
- **b.** IENF identification:
  - **i.** Frequently focus in and out to assist in fully visualizing all fibers present.
  - **ii.** IENF show punctate PGP9.5 immunostaining.
  - **iii.** Each individual profile is counted, regardless of whether it crosses the dermal/epidermal junction.
  - **iv.** Be aware of Langerhans cells, which are also located in the epidermis and PGP 9.5 +ve.
  - **v.** Langerhans cells appear as round cells with long, densely-stained, projections (Figure 4A) and should be tallied separately from IENF.

64 View the skin section on the computer via the digital camera using your imaging program of choice.

65 Trace the length of the dermal:epidermal junction over which you have counted IENF and SNP.

66 Report values as SNP/mm and IENF/mm.

BASIC PROTOCOL #7: Imaging Corneal nerves

Loss of sensory innervation of the cornea occurs in both diabetic patients (Quattrini et al., 2007) and mice (Chen et al., 2013). As visualization of corneal nerves by confocal microscopy is non invasive, it is becoming a popular biomarker for peripheral neuropathy that can be tracked iteratively during disease.

Materials

Retina Tomograph 3 with Rostock Cornea Module (Heidelberg Engineering Inc.)

Rostock Imaging Software (Heidelberg Engineering Inc.)

Tomocap (Heidelberg Engineering, Cat. #0220-001)

GenTeal gel (Novartis Pharmaceuticals Corp.)

Small animal platform (in house-manufactured)

Isoflurane vaporizer, regulator and delivery facemask

Exothermic hand warmer (Heat Factory)

Procedure

1. Anesthetize the animal within an induction chamber using 2.5–4.0 ppm isoflurane/oxygen mix.
   - **a.** On the small animal platform, this general anesthesia is maintained through the use of a facemask connected to the isoflurane regulator
   - **b.** If imaging takes longer than 5 minutes an exothermic crystallization hand warmer can be strapped onto the platform under the animal to maintain body temperature.
2. Placing the mouse onto the small animal platform:
   - **a.** Place the mouse on its side with its spine closest to the CCM objective and secure the body with one Velcro strap.
   - **b.** Turn the head until the chin is parallel to the platform and the eye closest to the CCM objective bulges slightly (Figure 5).
   - **c.** Gently secure the mouse's head into place using the second Velcro strap (Ensure that the strap is not tight as to restrict airway).
   - **d.** Place a generous amount of GenTeal eye gel on both eyes to create laser light coupling and to prevent the eyes drying.
3. Position the microscope objective near the center of the apex of the cornea
   - **a.** Ensure that the tomocap is touching the GenTeal gel but not the surface of the cornea
   - **b.** If the tomocap is pressing directly against the cornea the added pressure will create wrinkles on the corneal surface
4. Using the manual laser objective focus, withdraw the lens until the reflection of the light inside the Tomocap can be seen as an extremely bright glare
   - **a.** Press the reset button to reset the laser depth to zero
5. We collect images using the volume scan program that stores 40 sequential images. Individual and sequence images can also be collected using the

Rostock Imaging software. Consult the manufacturer's instructions for details.

6. Images exported from the Rostock Imaging Software are saved as individual TIFF files.

   a. Open these files in Preview in order to accurately and quickly scroll through the images in the correct order.

   b. Determine the sub-basal plexus:stromal junction by determining the last image of the sub-basal plexus and the first of the stromal layer:

      i. The sub-basal plexus is distinguished by its bright, reflective background and the presence of small linear nerve fibers throughout (Figure 6A).

      ii. The stromal layer is distinguished by its bright pyramidal-shaped keratocytes and large nerve fibers on a dark background (Figure 6B).

7. Each image, starting at the first visualizing the sub-basal nerve plexus, is quantified.

8. Overlie each image with an 8×8 grid (Figure 6C). We use an in-house program to merge the grid with the images.

9. Examine each square within the grid to make a yes/no determination on the presence of nerves within that square.

10. Once each square within the grid has been examined, record the amount of squares positively identified as containing nerves.

11. Repeat until every image from the first sub-basal plexus image to the last stromal layer image are quantified.

12. Data are presented as % occupancy using the following equation:

$$\%\,\text{nerve occupancy} = \left(\frac{\text{total\#boxes occupied by nerves in layer}}{\text{\#of images in layer} * \text{total\#of boxes in grid}}\right) * 100$$

9. SUPPORT PROTOCOLS

9.1 Motor function using the rotarod test

Stimulus-evoked behavioral tests such as the von Frey test (Basic Protocol #3) and the paw thermal test (Basic Protocol #5) that are interpreted as measures of sensory function should be accompanied by concurrent assessment of motor function, as impaired motor function could contribute to elongated withdrawal latencies from sensory stimuli. We use the protocol

described elsewhere in the Current Protocols in Mouse Biology as Basic Protocol 1 (Brooks et al., 2012) with the following modifications:

Materials

Rotarod device with 1.25 inch diameter mouse rods (Stoelting)

Procedure

1. Set acceleration rate at 4 rpm to 40 rpm over the first 120 seconds and a total rotation time of 300 seconds.
2. Set rod rotation to “backwards” so that mice have to advance towards the observer to stay on the rotating rod as it is helpful to watch their facial expressions as the revolutions increase.
3. Perform a single acclimation run.
4. Perform 3 consecutive tests for each mouse, recording time, maximal rpm and distance achieved. Use the median of the 3 tests to represent each parameter for each mouse.

10. REAGENTS AND SOLUTIONS

20% Paraformaldehyde (PFA), 2 L

Store at 4° C up to 12 months.

Total Preparation Time: approximately 5–7 hours

1. Microwave 1400 mL distilled water in a 2 L beaker for ~4 minutes or until just under 60° C.
2. Using a hot plate, maintain water temperature at 60° C – do not allow to heat past 60° C.
3. While stirring, add 400 g paraformaldehyde (PFA) in 4 ×100 g batches.
4. Allow ~30 minutes between each addition of PFA.
5. Do not expect the PFA to dissolve fully.
6. Continue to maintain temperature at 60° C.
7. Once all 400 g of PFA have been added and the solution has returned to 60° C, remove from heat.
8. Prepare a concentrated solution of sodium hydroxide: 150 mL distilled water + 50 g sodium hydroxide (NaOH). *This reaction is exothermic so add NaOH to water in small increments while stirring.*

9. While stirring, use a pipette to add all of the concentrated NaOH solution slowly to the PFA solution. *This will cause the PFA to go into solution.*
10. Place the beaker in an ice bath and cool to 25° C.
11. Place the beaker on the stir plate and measure the pH. It should be basic, around pH 11.
12. While stirring, use a pipette to add 12N hydrochloric acid (HCl) until the solution reaches pH 7.3. *The PFA solution should not contain any sediment at this point, but will remain cloudy.*
13. Vacuum filter the PFA solution using P2 filters. *Change the filter often, preferably before each refill of the Buchner funnel.*
14. The PFA solution should be clear after filtration.
15. Complete the volume to 2 L by adding distilled water.
16. Store at 4° C. *If the PFA precipitates out during storage, gently reheat the solution to 60° C while stirring.*

NOTE: Paraformaldehyde is highly toxic and sodium hydroxide and hydrochloric acid are highly caustic – perform all steps in a fume hood and wear a lab coat and gloves for the entire procedure.

NOTE: Collect all waste (solid and liquid) for disposal.

NOTE: By heating the polymer paraformaldehyde you are converting it into the monomer formaldehyde, a carcinogen.

4% Buffered Paraformaldehyde (PFA), 100 mL

Use on day of preparation only

1. In a beaker on a stir plate, combine:

   20 mL 20% Paraformaldehyde (see recipe)

   50 mL 0.2 M Sodium Phosphate Buffer (see recipe below)

   30 mL distilled water
2. Stir well, then aliquot as desired.

NOTE: Use ~10× more volume of 4% PFA compared to volume of tissue to ensure proper fixation.

5× Phosphate Buffered Saline (PBS), 1 L

Store at 4°C up to 12 months

1. In a beaker on a stir plate, combine:

1 L distilled water

6.0 g sodium phosphate dibasic (Na_2HPO_4)

1.1 g sodium phosphate monobasic (NaH_2PO_4)

42.5 g sodium chloride (NaCl)

2. Stir well to dissolve.

NOTE: If precipitation occurs over time, stir at room temperature or on low heat until dissolved.

1× Phosphate Buffered Saline (PBS)

Store at 4°C up to 12 months

1. In a beaker on a stir plate, combine:

   1 part 5× PBS

   4 parts distilled water

2. Stir well to combine.

0.2 M Sodium Phosphate Buffer, 1 L

Store at 4° C up to 12 months

1. In a beaker on a stir plate, combine:

   1 L distilled water

   28.4 g sodium phosphate dibasic

2. Stir until dissolved.

3. While stirring, add 0.2 M Sodium Phosphate Monobasic Buffer (see recipe) until the solution reaches pH 7.3.

4. Store at 4° C indefinitely, or until contaminants are seen.

NOTE: With time, crystals tend to form in 0.2 M Sodium Phosphate Buffer. If this happens, stir at room temperature or on low heat until the crystals are fully dissolved before using the buffer.

0.2 M Sodium Phosphate Monobasic Buffer, 1 L

Store at 4° C up to 12 months

1. In a beaker on a stir plate, combine:

   1 L distilled water

   27.6 g sodium phosphate monobasic

2. Stir until dissolved.

3. Store at 4° C indefinitely, or until contaminants are seen.

Resin

Use on day of preparation only

1. Calculate the amount of resin needed for the 50%-50% propylene oxide-resin incubation (step 10), 100% resin incubation (step 11) and production of resin blocks (~0.5 mL per mold well).
2. Mark lines on a plastic disposable beaker for 50%, 80%, and 100% of the total volume.
3. Add DDSA resin up to the 50% line.
4. Add araldite resin up to the 80% line.
5. Add Embed 812 resin up to the 100% line.
6. Stir for 5 minutes.
7. Add 1.6 mL of DMP-30 catalyst for each 100 mL of resin mixture. Stir for 15 minutes.
8. The mixture is now ready for use.

11. COMMENTARY

Background Information

Mice are now a widely studied model of diabetic neuropathy that exhibit a number of disorders shared with the human condition (Biessels et al., 2014).

Conduction Velocity—NCV slowing in large myelinated sensory and motor fibers has been extensively validated as an early, sensitive and predictive indication of diabetic neuropathy for both diagnosis of disease and assessment of progression in clinical trials. It can be measured repeatedly over time and protocols can be standardized between sites with analysis performed off-line at a central site. A combination of biochemical and structural features of diabetic neuropathy likely contribute to NCV slowing in diabetic patients. However, NCV slowing is not a direct measure of small fiber function or structure so may not detect efficacy of therapeutics that specifically target small-fibers.

The use of NCV slowing as the gold standard for diagnosis of neuropathy and the primary determinant of therapeutic efficacy in clinical trials has driven extensive study of nerve conduction in rodent models of diabetes. NCV slowing in diabetic rodents is detectable within weeks of onset of diabetes and appears to comprise an acute onset, readily reversible “metabolic” component and a slowly developing “structural” component that is more resistant to rapid reversal. Many therapies are effective in preventing or reversing the acute NCV slowing that develops after 2–12 weeks of diabetes in rodents. However, translation to clinical efficacy and regulatory approval has not been achieved, possibly because NCV slowing in diabetic subjects includes aspects of nerve pathology that may not be amenable to immediate metabolic intervention such as segmental demyelination and axonal loss. The value of NCV slowing in phenotyping diabetic neuropathy in mice should therefore be

tempered with cautious interpretation, as mechanisms underlying the phenomenon may not be identical in mice and humans.

Inferring Sensory Neuropathy from Behavioral Tests—Patients with diabetic neuropathy describe numbness in the hands and feet and/or abnormal sensations ranging from occasional tingling to persistent burning or lancinating pain. Although subjective, these symptoms can be quantified using responses to descriptive questionnaires and rating devices such as the visual analog scale (VAS). It is also possible to obtain more objective measures of sensory function using psychophysical tests that measure perception and pain perception thresholds to external stimuli such a temperature, touch and vibration. Such tests are codified as quantitative sensory testing (Maier et al., 2010).

As mice cannot report their perceptions, the majority of preclinical studies assess aversive behaviors in response to noxious or non-noxious stimuli to represent measures of sensory loss or pain. There have also been attempts to use changes in natural behaviors such as facial expressions (Langford et al., 2010). Measuring response times or thresholds has parallels in the clinical QST battery and the common methods that are used in diverse rodent models of neuropathic pain have been extensively described elsewhere in the Current Protocols in Mouse Biology series. Of the many behavioral tests available, we prefer those that use touch and thermal stimuli, as they most closely reflect aspects of the clinical QST and do not require animal restraint. We also use the formalin test in rats, where it can give information about persistent activation of peripheral and spinal sensory processing. However, diabetic mice do not respond to paw formalin injection (Lee-Kubli et al., 2014). There are a number of other potentially useful behavioral tests that have yet to be fully validated in diabetic mice.

Pathology in Nerve Trunks—Peripheral nerve biopsies are not commonly performed in diabetic patients, as they are invasive and unnecessary for diagnostic purposes. However, sural nerves have historically been collected from diabetic subjects for research and clinical trial purposes. Such biopsies show demyelination, axonal degeneration and clusters of regenerating axons within the peripheral nerve trunk, along with changes to endoneurial blood vessels and the perineurium (Kalichman et al., 1998; Powell et al., 1985). Reduced mean fiber diameter and a trend to fiber loss have been reported in distal sensory nerves of long-term STZ-diabetic mice (Kennedy and Zochodne, 2005), while motor neurons may retract from the neuromuscular junction (Ramji et al., 2007).

Epidermal nerves—Skin biopsies have emerged as a means of visualizing and quantifying distal portions of peripheral nerves in diabetic patients that is less invasive than sural nerve biopsy and allows repeated assessment of nerve structure over time. Guidelines suggest immunostaining against the pan-neuronal marker PGP9.5 followed by quantification of axons that cross the dermal:epidermal junction (Lauria et al., 2010). The derived measure of intra-epidermal nerve fibers (IENF, quantified in #/mm length of dermal:epidermal border assessed) is reduced in patients with both type 1 and type 2 diabetes and also those with metabolic syndrome, supporting the claim that this measurement represents an early and sensitive manifestation of distal small fiber sensory neuropathy. Dermal somatic nerves and autonomic nerves innervating sweat glands are also captured in skin biopsies and can be

quantified (Gibbons et al., 2010). It is tempting to view IENF depletion as a structural correlate to loss of thermal nociception, as depletion of IENF in normal subjects exposed to capsaicin induces loss of heat sensation. However, as individual sensory axons that cross into the epidermis undergo branching and may have territories that overlap with adjacent axons, a linear relationship between IENF density and sensory function should not be assumed. Indeed, there is no loss of heat sensation in human subjects that lost less than 50% of PGP9.5 +ve IENF following capsaicin treatment (Malmberg et al., 2004), suggesting a step function rather than linearity.

Skin samples from diabetic mice also show IENF depletion. However, loss of thermal nociception can precede detectable loss of PGP9.5+ve IENF in STZ-diabetic mice (Beiswenger et al., 2008a), suggesting that the functional consequences of IENF depletion should be interpreted with caution and that other factors may contribute to early loss of thermal nociception in diabetic mice. Whether reduced IENF density in diabetes represents active degeneration or controlled terminal arbor reorganization also remains uncertain. PGP9.5 is a cytoplasmic protein (ubiquitin carboxy-terminal hydrolase L1) and any reduction in staining could potentially reflect reduced protein expression rather than loss of axon structure. However, reduced density of PGP9.5 immunostained axons in diabetic mice corresponds to a similar depletion when immunostained for the structural protein tau (Beiswenger et al., 2008b). Sophisticated studies have immunostained for markers of specific sub-classes of sensory neurons, and it is plausible that the apparent lack of linearity between IENF depletion and loss of thermal nociception seen using a pan-neuronal marker could mask a more subtle association with select sub-types of sensory neuron (Johnson et al., 2008). The large array of antibodies now available that are directed at mouse epitopes makes many new and incisive studies viable.

Imaging corneal nerves in mice—Confocal microscopes that focus on the front of the eye allow imaging of corneal sensory nerves that is non-invasive and does not require contrast agents. Iterative measurements can therefore be performed on diabetic subjects for longitudinal studies of disease progression and response to therapeutic intervention. Reduced corneal nerve density in diabetic subjects is a sensitive biomarker of peripheral neuropathy that compares favorably with other structural, functional and symptom-based measures (Quattrini et al., 2007). The corneal confocal microscope can also be used to follow progressive depletion of corneal nerves in diabetic rats and mice (Chen et al., 2013). At present, it is not clear whether depletion of corneal nerve density in diabetic rodents represents active degeneration or reorganization.

Critical Parameters

Mice with STZ-induced type 1 diabetes can revert to normoglycemia after months of hyperglycemia, while type 2 diabetic db/db mice eventually develop insulinopenia. The general cachexia associated with severe or prolonged diabetes can impede interpretation of behavioral tests. It is therefore important to be aware of the metabolic and behavioral phenotype of diabetic mice throughout the study period, particularly at time points when neuropathy is measured. We make weekly measurements of body weight as an index of general health and of blood glucose as an index of diabetes. We also measure rotarod

performance whenever tests of aversive behaviors are performed to determine the extent that motor dysfunction could contribute to apparent sensory loss. Blood HbA1c and plasma insulin levels are measured at the end of a study using commercial assay kits to build a more complete picture of the diabetic condition. Other parameters, such a plasma lipid profile, may also be helpful for mechanistic studies.

Many of the indices of neuropathy suffer from inherent biological variability that can be compounded by small variations in assay procedures. We therefore assign only one person to any particular assay and ensure that, whenever possible, that they perform the assay at all time points throughout a study period. This is particularly important for behavioral assays and for morphometric analyses of nerves. It is also critical to blind observers during behavioral assays and to code all tissues and images before analyses, although the physical consequences of type 1 and type 2 diabetes can make the former challenging.

Troubleshooting

Mouse strains for STZ-induced diabetes—For any given dose of STZ administered, outbred strains such as Swiss Webster tend to be more tolerant of STZ-induced diabetes, with higher initial survival rates, less weight loss and longer survival times than inbred mice such as C57 derivatives. Onset of neuropathy in outbred mice may be correspondingly slower and less dramatic. As plasma glucose levels are generally similar across strains when given STZ, relatively less severe insulinopenia may contribute to the improved health status and milder neuropathy of outbred strains. Choice of mouse strain may also be dictated by availability of a specific genetic manipulation of interest onto which diabetes is to be superimposed. At present, we favor Swiss Webster mice for studies of long-term diabetes and C57Bl/6 mice when superimposing diabetes onto transgenic or knock-out mice.

Maintenance of STZ-diabetic mice—High doses of STZ kill pancreatic β cells by entering via the GLUT-2 transporter and generating free radicals that damage DNA. This prompts attempted repair by poly-ADP ribose polymerase and consequent depletion of cellular NADH, precipitating cell death by apoptosis (Wada and Yagihashi, 2004). As cells undergo apoptosis they release their stored insulin, causing transient hyperinsulinemia and hypoglycemia (unfasted blood glucose levels below 5 mmol/L). Occasional deaths of STZ-injected mice may occur during this period. Some laboratories attempt to mitigate this transient hypoglycemia by providing glucose solutions for the first 3 days after STZ injection, either as bolus ip injections or via drinking water. We have used this approach for STZ-injected rats and alloxan-injected rabbits (20% glucose solution *ad libitum*) with varied success, but generally do not do so for mice when using the STZ injection regime described above. After confirmation of hyperglycemia, mice become polyphagic (eat up to 2–3 times that of control mice), polydypsic (increase water consumption 3–4 fold) and polyuric so that they require additional food, extra water bottles and daily replacement of soiled bedding. Diabetic mice should be observed daily and weighed weekly. Mice showing abnormal behavior such as reduced locomotion and withdrawing from their social group, or loss of more than 20% of starting body weight, may be candidates for trace insulin supplementation to prevent cachexia and prolong life. Trace insulin replacement is achieved by sub-cutaneous placement of one slow release insulin pellet (LinBit, Linshin, Canada) into an isoflurane-

anesthetized mouse following the manufacturers protocol. The intent is to relieve catabolic dominance without impacting hyperglycemia. Each pellet is active for approximately 40 days before replacement and body weight is tracked as an index of insulin pellet efficacy. Animals that remain within 20% of starting body weight are considered acceptable for continued study, while those that do not respond are euthanized. Local and national laws may require different procedures and protocols under development should be discussed with the local IACUC.

STZ Toxicity—There have been intermittent claims that STZ has direct neurotoxic effects that can impede interpretation of the pathogenesis of nerve disorders in STZ-diabetic rodents. There is certainly a degree of acute nephrotoxicity associated with high doses of STZ that prompted development of multiple low dose STZ injection regimes (Breyer et al., 2005). Cells expressing the GLUT-2 glucose transporter such as pancreatic β cells and hepatocytes are most liable to acute STZ toxicity. Neuronal expression of GLUT-2 is limited to the glucose sensing cells of the hypothalamus and basal medulla that are involved in thermoregulation and leptin sensitivity (Mounien et al., 2010). This makes direct effects on peripheral nerve unlikely. STZ is also rapidly metabolized and cleared from the body within hours, so that any immediate and direct chemical effects of STZ resolve long before behavioral and physiological indices of neuropathy appear. Reports of STZ-injected animals that develop behavioral disorders without ever becoming hyperglycemic have been associated with STZ-induced insulin depletion that was not severe enough to promote persistent hyperglycemia (Romanovsky et al., 2006) while inbred and outbred strains of mice co-injected with STZ and excess 6-O-methyl glucose to prevent STZ-uptake by GLUT-2 transporters developed neither diabetes nor neuropathy when compared to mice given STZ-alone (Davidson et al., 2009). Finally, as noted above, indices of neuropathy in STZ-injected animals are replicated in other models of type 1 and type 2 diabetes. Thus, while all data obtained in STZ-injected mice should be interpreted with appropriate caution, indices of peripheral neuropathy that develop only weeks-months after onset of diabetes are unlikely to be caused by an earlier acute and transient exposure to systemic STZ *per se*. Nevertheless, the provenance of all newly-identified disorders in STZ diabetic rodents should always be confirmed by demonstrating that they can be prevented and reversed by insulin replacement therapy, as demonstrated for tactile allodynia (Calcutt et al., 1996).

Genetic Models of Type 2 diabetes—While genetic models of type 2 diabetes such as the db/db and ob/ob mice are not tainted by potential toxicity of inducing agents there are a number of other caveats to consider, not least that they represent knockout of leptin or it's receptor and thus have a broad physiological impairment that is not a feature of diabetes *per se*. Both models also eventually progress to β cell failure and thus insulin deficiency after around 6 months and can become quickly moribund as acute type 1 diabetes is superimposed upon chronic type 2 diabetes. We have frequently noted that some indices of neuropathy in models of type 2 diabetes remain mild until the progression to concurrent type 1 diabetes begins. It is therefore important to carefully phenotype not only neuropathy but also the general physiology of these models before beginning to ascribe causality to type 2 diabetes.

Nerve conduction velocity—We use near nerve stimulation of the sciatic nerve in rodents using needle electrodes with recording of the resultant compound muscle action potentials (CMAP: Figure 1) from muscles of the ipsialteral foot that allows recording of both motor (M) waves arising from orthodromic stimulation and sensory (H-reflex) waves arising from orthodromic stimulation of sensory nerves followed by a spinal reflex and activation of motor neurons. These procedures are similar to those used clinically, although the latter routinely employ surface electrodes. Clinical studies also identify F waves, which represent antidromic stimulation of motor axons to the ventral horn then a rebound orthodromic stimulation of the same axons, but in our experience these are rarely seen in rodents. Identification of the H wave can be confirmed by its distinct pattern of emergence and decline when increasing stimulation voltage compared to M and F waves, a frequently different shape compared to the M wave and, for validation purposes, its disappearance when the dorsal root is selectively transected or anesthetized. Direct nerve recording and single fiber recordings are also viable in rodents. We do not measure CMAP amplitude as an index of fiber recruitment in rodents as we find it to be unreliable due to variability depending on electrode placement, animal respiratory movements and, for the H wave in particular, depth of anesthesia. Other technical considerations include maintaining a constant and defined nerve temperature (37–38°C) between animals, as NCV changes by around 2.5 m/s/°C (Lee-Kubli et al., 2014) and ensuring that we measure NCV at least at onset and termination of a study, to establish whether diabetes-induced defects in NCV are ascribed to an absolute decrease from onset or impairment of growth related increases over time (Calcutt, 2004). We use the same technique for rats and mice, although obtaining H waves to determine sensory NCV can be challenging in mice, due to less subtle control of anesthesia. The volatile anesthetic isoflurane allows regular iterative measurements during a longitudinal study as diabetic mice recover quickly after anesthesia is withdrawn and deaths are rare. Injectable anesthetics may be used in terminal studies and can make detection of H waves more reliable.

Behavioral Tests—When a new index of pain is identified, confidence in its validity is increased when a treatment can restore normal stimulus-evoked behavioral responses to stimuli without improving muscle mass at the stimulation site. In contrast, we are particularly cautious when identifying a new aspect of apparent sensory loss if the cohort also shows impaired motor function in the rotarod test (Support Protocol #9.1) and develop confidence only when a therapeutic intervention can restore sensory function without improving motor function. Practical modifications to the common behavioral tests of motor and sensory function that are specific to diabetic mice include not leaving animals in a testing apparatus without access to water for more than 60 minutes, as they can rapidly develop dehydration that affects behavior, and also being persistent in removing urine from the surface of testing devices as this will alter transduction properties of the surface and can provide a distraction to mice that is less prevalent in controls. Consequently, performing behavioral tests on diabetic mice can be even more challenging than when using non-diabetic mice, as the usual habituation and measurement periods can be constantly interrupted. Additional caveats to measurement and interpretation of sensory tests in diabetic mice, beyond those of whether the tests illustrate perception of pain in the human sense, require consideration. Perhaps the most important is the health status of diabetic mice,

recognizing that they have a systemic disease that affects many tissues and organs. Mice with insulinopenia or prolonged insulin resistance will undergo muscle wasting and extreme cases show marked behavioral depression that can impede response times and can lead to misinterpretation as sensory loss. These issues can be somewhat mitigated by using trace insulin replacement therapy to prevent excessive catabolic dominance – while recognizing that trace insulin can improve nerve function and structure in diabetic rodents independent of glycemic control (Guo et al., 2011). Conversely, obesity in type 2 diabetic mice also impairs free movement during walking or swimming. Our approach is to observe animals daily for abnormal motor behavior in their home cage and to weigh them weekly. Diabetic mice that show withdrawn behavior or with persistent cachexia (weight loss of >20% of starting weight over 2–3 weeks) are removed from a cohort. The rotarod test of motor function (Support Protocol #9.1) is also performed to confirm that the capacity to respond to stimuli is intact.

Large Fiber Pathology—Unfortunately, many published reports of overt nerve pathology in short-term (weeks-months) diabetic mice illustrate common artifacts associated with nerve extraction, fixation and processing and should be treated with caution. For the best preservation of myelin, mid-thigh sciatic nerve or its more distal (sural, tibial, common peroneal) branches are taken at autopsy, fixed by perfusion or immersion and processed to resin blocks. This provides excellent preservation of all cellular and sub-cellular structures, including myelin lamellae and mitochondria, when viewed by light (Figure 2) or electron microscopy. We use sections cut from resin blocks for quantifying epineurial and endoneurial blood vessel numbers, myelinated fiber density, axonal caliber and myelin thickness using bright field light microscopy and computer-assisted morphometry. Cross sections of individual fibers that contain the paranodal region, Schmidt-Lanterman incisures or Schwann cell nuclei are not quantified. While these are all normal features of well-preserved nerves and do not represent pathology, they do inherently distort axon and/or myelin dimensions. We do not process nerve to paraffin blocks for nerve morphometry as, while such material allows spatial distribution of specific antigens to be visualized using immunocytochemistry and protein density estimated by densitometry, there is poor retention of nerve morphology with myelin being particularly disrupted.

Intra-Epidermal Nerve Fibers—There is variability between research groups in how IENF are viewed and quantified in skin from mice. Some follow the clinical standard that counts PGP9.5 immunopositive axons as they cross the dermal:epidermal junction (Lauria et al., 2010), which has the virtues of simplicity and clinical equivalence. However, this approach does not account for early retraction of axon terminals or for re-organization of the terminal arbors and receptive fields within the epidermis that are most pertinent to thermal nociception. This approach requires sections thick enough to allow all axons to be traced over sufficient length to be seen to cross the dermal:epidermal junction without passing out of view (Figure 4B). For research purposes, we have favored use of thinner sections and light microscopy to count all PGP9.5 immunostained axon fragments in the epidermis (Figure 4A). This method does not report axon number, as any one axon may be counted many times as it passes in and out of view, but allows a relatively quick and reproducible estimation of axon density in the epidermis that is likely to be sensitive to early shifts in

terminal arborization prior to retraction beyond the dermal:epidermal junction. It also allows visual discrimination between axons and the processes of dendritic Langerhans' cells (Figure 4A), which are also PGP 9.5 immunopositive and can distort presumptive IENF counts (Doss and Smith, 2012).

Corneal Sensory Nerves—In small species such as the mouse, the distal portions of corneal nerves are fine and move between different planes of section (Figure 6A), which precludes accurate measurement of nerve branching and other features that are viable in thicker human corneal nerves (Chen et al., 2013; Quattrini et al., 2007). A number of alternative approaches have therefore been developed by research laboratories. We use the ability of the Heidelberg Retina Tomograph with Rostok Cornea Module to capture 40 sequential images at 2μm intervals from the corneal epithelium to the mid stromal region and use this volume scan to quantify nerve occupancy (Figure 6C) at each anatomic position passing from Bowman's layer to the stroma (Chen et al., 2013). Another approach measures total visible nerve length per unit area in selected images within a specific layer of the cornea (Yorek et al., 2014).

Anticipated Results

Onset and progression of diabetes and neuropathy can vary by mouse model, by mouse strain within a particular model and by the severity of insulin deficiency and/or hyperglycemia within a particular study. Consequently, appropriate age, strain and sex matched control animals should accompany every study. Data obtained from a study in adult female C57 Bl/6J mice treated with STZ (90 mg/kg/day on 2 consecutive days) are shown to illustrate the neuropathy phenotype that can be expected (Table 1 and Figure 7). These mice developed mild type 1 diabetes, as indicated by a small decline in body weight and elevated blood glucose (Table 1). Rotarod performance was normal, indicating no motor dysfunction that would contribute to apparent sensory loss in aversive behavioral tests. After 8 weeks of diabetes, large fiber dysfunction is indicated by significant motor NCV slowing and allodynia (lower response thresholds) to both manual and electronic von Frey filaments (Figure 7A). Small fiber neuropathy is illustrated by paw thermal hypoalgesia (increased response time and temperature), reduced IENF density in paw skin and reduced nerve occupancy in the cornea (Figure 7B). All of these disorders are features of human diabetic neuropathy, including the occurrence of both indices of sensory loss (thermal hypoalgesia) and increased pain perception (allodynia to the light touch of manual von Frey filaments and pressure applied by the electronic von Frey filament). Loss of thermal sensation was accompanied by structural neuropathy of small sensory fibers in the paw skin and cornea, but the temptation to assume causality – that fiber loss caused loss of thermal sensation – should be resisted without more definitive data.

Time Considerations

When planning a diabetic neuropathy phenotyping or drug therapy study, we start with a cohort of no more than 60 animals that can be divided into as many control and diabetic groups as required. This allows full behavioral (manual and electronic von Frey tests, paw heat test, rotarod test), physiological (nerve conduction) and histological (corneal nerve) phenotyping of all animals to be completed within 5 working days. Behavioral tests are

performed at the start of the week prior to those that require anesthesia but are non-invasive (corneal confocal microscopy) and finally anesthesia with minor tissue invasion (nerve conduction velocity). We usually perform this sequence of tests once every four weeks for the duration of a study, although more frequent testing is viable as required. After the last testing sequence, animals are killed and tissue processed for histology and morphometry, which can take an additional 1–2 months. Thus, in a study planned to span 6 months of diabetes, we would conservatively allow 9 months from ordering animals and allowing them to acclimate to completing analysis of the entire data set.

Acknowledgments

Supported by NIH grants DK102032 and NS081082 (both NAC) and AG039736 (CGJ).

LITERATURE CITED

Anderson NJ, King MR, Delbruck L, Jolivalt CG. Role of insulin signaling impairment, adiponectin and dyslipidemia in peripheral and central neuropathy in mice. Dis Model Mech. 2014; 7:625–633. [PubMed: 24764191]

Beiswenger KK, Calcutt NA, Mizisin AP. Dissociation of thermal hypoalgesia and epidermal denervation in streptozotocin-diabetic mice. Neurosci Lett. 2008a; 442:267–272. [PubMed: 18619518]

Beiswenger KK, Calcutt NA, Mizisin AP. Epidermal nerve fiber quantification in the assessment of diabetic neuropathy. Acta Histochem. 2008b; 110:351–362. [PubMed: 18384843]

Biessels GJ, Bril V, Calcutt NA, Cameron NE, Cotter MA, Dobrowsky R, Feldman EL, Fernyhough P, Jakobsen J, Malik RA, Mizisin AP, Oates PJ, Obrosova IG, Pop-Busui R, Russell JW, Sima AA, Stevens MJ, Schmidt RE, Tesfaye S, Veves A, Vinik AI, Wright DE, Yagihashi S, Yorek MA, Ziegler D, Zochodne DW. Phenotyping animal models of diabetic neuropathy: a consensus statement of the diabetic neuropathy study group of the EASD (Neurodiab). J Peripher Nerv Syst. 2014; 19:77–87. [PubMed: 24934510]

Bour-Jordan H, Thompson HL, Giampaolo JR, Davini D, Rosenthal W, Bluestone JA. Distinct genetic control of autoimmune neuropathy and diabetes in the non-obese diabetic background. J Autoimmun. 2013; 45:58–67. [PubMed: 23850635]

Breyer MD, Bottinger E, Brosius FC 3rd, Coffman TM, Harris RC, Heilig CW, Sharma K, Amdcc. Mouse models of diabetic nephropathy. J Am Soc Nephrol. 2005; 16:27–45. [PubMed: 15563560]

Brooks SP, Trueman RC, Dunnett SB. Assessment of Motor Coordination and Balance in Mice Using the Rotarod, Elevated Bridge, and Footprint Tests. Curr Protoc Mouse Biol. 2012; 2:37–53. [PubMed: 26069004]

Calcutt NA. Modeling diabetic sensory neuropathy in rats. Methods Mol Med. 2004; 99:55–65. [PubMed: 15131329]

Calcutt NA, Freshwater JD, Mizisin AP. Prevention of sensory disorders in diabetic Sprague-Dawley rats by aldose reductase inhibition or treatment with ciliary neurotrophic factor. Diabetologia. 2004; 47:718–724. [PubMed: 15298349]

Calcutt NA, Jorge MC, Yaksh TL, Chaplan SR. Tactile allodynia and formalin hyperalgesia in streptozotocin-diabetic rats: effects of insulin, aldose reductase inhibition and lidocaine. Pain. 1996; 68:293–299. [PubMed: 9121817]

Calcutt NA, Willars GB, Tomlinson DR. Statil-sensitive polyol formation in nerve of galactose-fed mice. Metabolism. 1988; 37:450–453. [PubMed: 3130544]

Chaplan SR, Bach FW, Pogrel JW, Chung JM, Yaksh TL. Quantitative assessment of tactile allodynia in the rat paw. J Neurosci Methods. 1994; 53:55–63. [PubMed: 7990513]

Chen DK, Frizzi KE, Guernsey LS, Ladt K, Mizisin AP, Calcutt NA. Repeated monitoring of corneal nerves by confocal microscopy as an index of peripheral neuropathy in type-1 diabetic rodents and the effects of topical insulin. J Peripher Nerv Syst. 2013; 18:306–315. [PubMed: 24147903]

Davidson E, Coppey L, Lu B, Arballo V, Calcutt NA, Gerard C, Yorek M. The roles of streptozotocin neurotoxicity and neutral endopeptidase in murine experimental diabetic neuropathy. Exp Diabetes Res. 2009; 2009:431980. [PubMed: 20148083]

Dirig DM, Salami A, Rathbun ML, Ozaki GT, Yaksh TL. Characterization of variables defining hindpaw withdrawal latency evoked by radiant thermal stimuli. J Neurosci Methods. 1997; 76:183–191. [PubMed: 9350970]

Doss AL, Smith PG. Nerve-Langerhans cell interactions in diabetes and aging. Histol Histopathol. 2012; 27:1589–1598. [PubMed: 23059889]

Gibbons CH, Illigens BM, Wang N, Freeman R. Quantification of sudomotor innervation: a comparison of three methods. Muscle Nerve. 2010; 42:112–119. [PubMed: 20544913]

Grote CW, Groover AL, Ryals JM, Geiger PC, Feldman EL, Wright DE. Peripheral nervous system insulin resistance in ob/ob mice. Acta Neuropathol Commun. 2013; 1:15. [PubMed: 24252636]

Guilford BL, Ryals JM, Wright DE. Phenotypic changes in diabetic neuropathy induced by a high-fat diet in diabetic C57BL/6 mice. Exp Diabetes Res. 2011; 2011:848307. [PubMed: 22144990]

Guo G, Kan M, Martinez JA, Zochodne DW. Local insulin and the rapid regrowth of diabetic epidermal axons. Neurobiol Dis. 2011; 43:414–421. [PubMed: 21530660]

Johnson MS, Ryals JM, Wright DE. Early loss of peptidergic intraepidermal nerve fibers in an STZ-induced mouse model of insensate diabetic neuropathy. Pain. 2008; 140:35–47. [PubMed: 18762382]

Kalichman MW, Powell HC, Mizisin AP. Reactive, degenerative, and proliferative Schwann cell responses in experimental galactose and human diabetic neuropathy. Acta Neuropathol. 1998; 95:47–56. [PubMed: 9452821]

Kennedy JM, Zochodne DW. Experimental diabetic neuropathy with spontaneous recovery: is there irreparable damage? Diabetes. 2005; 54:830–837. [PubMed: 15734862]

Khan GM, Chen SR, Pan HL. Role of primary afferent nerves in allodynia caused by diabetic neuropathy in rats. Neuroscience. 2002; 114:291–299. [PubMed: 12204199]

Langford DJ, Bailey AL, Chanda ML, Clarke SE, Drummond TE, Echols S, Glick S, Ingrao J, Klassen-Ross T, Lacroix-Fralish ML, Matsumiya L, Sorge RE, Sotocinal SG, Tabaka JM, Wong D, van den Maagdenberg AM, Ferrari MD, Craig KD, Mogil JS. Coding of facial expressions of pain in the laboratory mouse. Nat Methods. 2010; 7:447–449. [PubMed: 20453868]

Lauria G, Hsieh ST, Johansson O, Kennedy WR, Leger JM, Mellgren SI, Nolano M, Merkies IS, Polydefkis M, Smith AG, Sommer C, Valls-Sole J, European Federation of Neurological, S; Peripheral Nerve, S. European Federation of Neurological Societies/Peripheral Nerve Society Guideline on the use of skin biopsy in the diagnosis of small fiber neuropathy. Report of a joint task force of the European Federation of Neurological Societies and the Peripheral Nerve Society. Eur J Neurol. 2010; 17:903–912. e944–909. [PubMed: 20642627]

Lee-Kubli CA, Mixcoatl-Zecuatl T, Jolivalt CG, Calcutt NA. Animal models of diabetes-induced neuropathic pain. Curr Top Behav Neurosci. 2014; 20:147–170. [PubMed: 24510303]

Leiter EH, Schile A. Genetic and Pharmacologic Models for Type 1 Diabetes. Curr Protoc Mouse Biol. 2013; 3:9–19. [PubMed: 24592352]

Lutz TA, Woods SC. Overview of animal models of obesity. Curr Protoc Pharmacol. 2012 Chapter 5:Unit5 61.

Maier C, Baron R, Tolle TR, Binder A, Birbaumer N, Birklein F, Gierthmuhlen J, Flor H, Geber C, Huge V, Krumova EK, Landwehrmeyer GB, Magerl W, Maihofner C, Richter H, Rolke R, Scherens A, Schwarz A, Sommer C, Tronnier V, Uceyler N, Valet M, Wasner G, Treede RD. Quantitative sensory testing in the German Research Network on Neuropathic Pain (DFNS): somatosensory abnormalities in 1236 patients with different neuropathic pain syndromes. Pain. 2010; 150:439–450. [PubMed: 20627413]

Malmberg AB, Mizisin AP, Calcutt NA, von Stein T, Robbins WR, Bley KR. Reduced heat sensitivity and epidermal nerve fiber immunostaining following single applications of a high-concentration capsaicin patch. Pain. 2004; 111:360–367. [PubMed: 15363880]

Mansford KR, Opie L. Comparison of metabolic abnormalities in diabetes mellitus induced by streptozotocin or by alloxan. Lancet. 1968; 1:670–671. [PubMed: 4170654]

Minett MS, Quick K, Wood JN. Behavioral Measures of Pain Thresholds. Curr Protoc Mouse Biol. 2011; 1:383–412. [PubMed: 26068997]

Mounien L, Marty N, Tarussio D, Metref S, Genoux D, Preitner F, Foretz M, Thorens B. Glut2-dependent glucose-sensing controls thermoregulation by enhancing the leptin sensitivity of NPY and POMC neurons. FASEB J. 2010; 24:1747–1758. [PubMed: 20097878]

Powell HC, Rosoff J, Myers RR. Microangiopathy in human diabetic neuropathy. Acta Neuropathol. 1985; 68:295–305. [PubMed: 4090941]

Quattrini C, Tavakoli M, Jeziorska M, Kallinikos P, Tesfaye S, Finnigan J, Marshall A, Boulton AJ, Efron N, Malik RA. Surrogate markers of small fiber damage in human diabetic neuropathy. Diabetes. 2007; 56:2148–2154. [PubMed: 17513704]

Ramji N, Toth C, Kennedy J, Zochodne DW. Does diabetes mellitus target motor neurons? Neurobiol Dis. 2007; 26:301–311. [PubMed: 17337195]

Romanovsky D, Cruz NF, Dienel GA, Dobretsov M. Mechanical hyperalgesia correlates with insulin deficiency in normoglycemic streptozotocin-treated rats. Neurobiol Dis. 2006; 24:384–394. [PubMed: 16935517]

Schenone AE, Dyck PJ. Which endoneurial microvessel histologic measurements are least influenced by vasomotor tone? Brain Res. 1987; 402:151–154. [PubMed: 3828781]

Tomlinson DR, Gardiner NJ. Glucose neurotoxicity. Nat Rev Neurosci. 2008; 9:36–45. [PubMed: 18094705]

Wada R, Yagihashi S. Nitric oxide generation and poly(ADP ribose) polymerase activation precede beta-cell death in rats with a single high-dose injection of streptozotocin. Virchows Arch. 2004; 444:375–382. [PubMed: 14762714]

Wahren J, Larsson C. C-peptide: new findings and therapeutic possibilities. Diabetes Res Clin Pract. 2015; 107:309–319. [PubMed: 25648391]

Xu QG, Li XQ, Kotecha SA, Cheng C, Sun HS, Zochodne DW. Insulin as an in vivo growth factor. Exp Neurol. 2004; 188:43–51. [PubMed: 15191801]

Yeomans DC, Pirec V, Proudfit HK. Nociceptive responses to high and low rates of noxious cutaneous heating are mediated by different nociceptors in the rat: behavioral evidence. Pain. 1996; 68:133–140. [PubMed: 9252008]

Yeomans DC, Proudfit HK. Nociceptive responses to high and low rates of noxious cutaneous heating are mediated by different nociceptors in the rat: electrophysiological evidence. Pain. 1996; 68:141–150. [PubMed: 9252009]

Yorek MS, Obrosov A, Shevalye H, Lupachyk S, Harper MM, Kardon RH, Yorek MA. Effect of glycemic control on corneal nerves and peripheral neuropathy in streptozotocin-induced diabetic C57Bl/6J mice. J Peripher Nerv Syst. 2014; 19:205–217. [PubMed: 25403729]

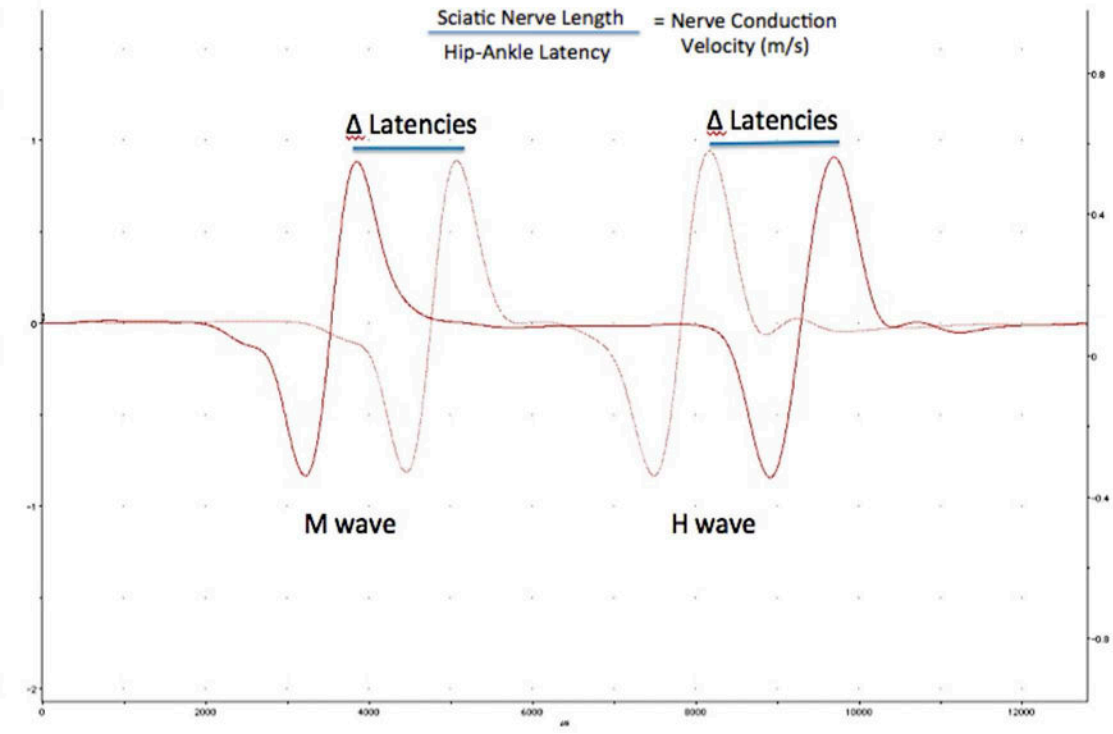

Figure 1.

Typical traces recorded after stimulation at the ankle (solid line) and at the hip (dashed line), depicting latencies between stimulations (Δ latencies).

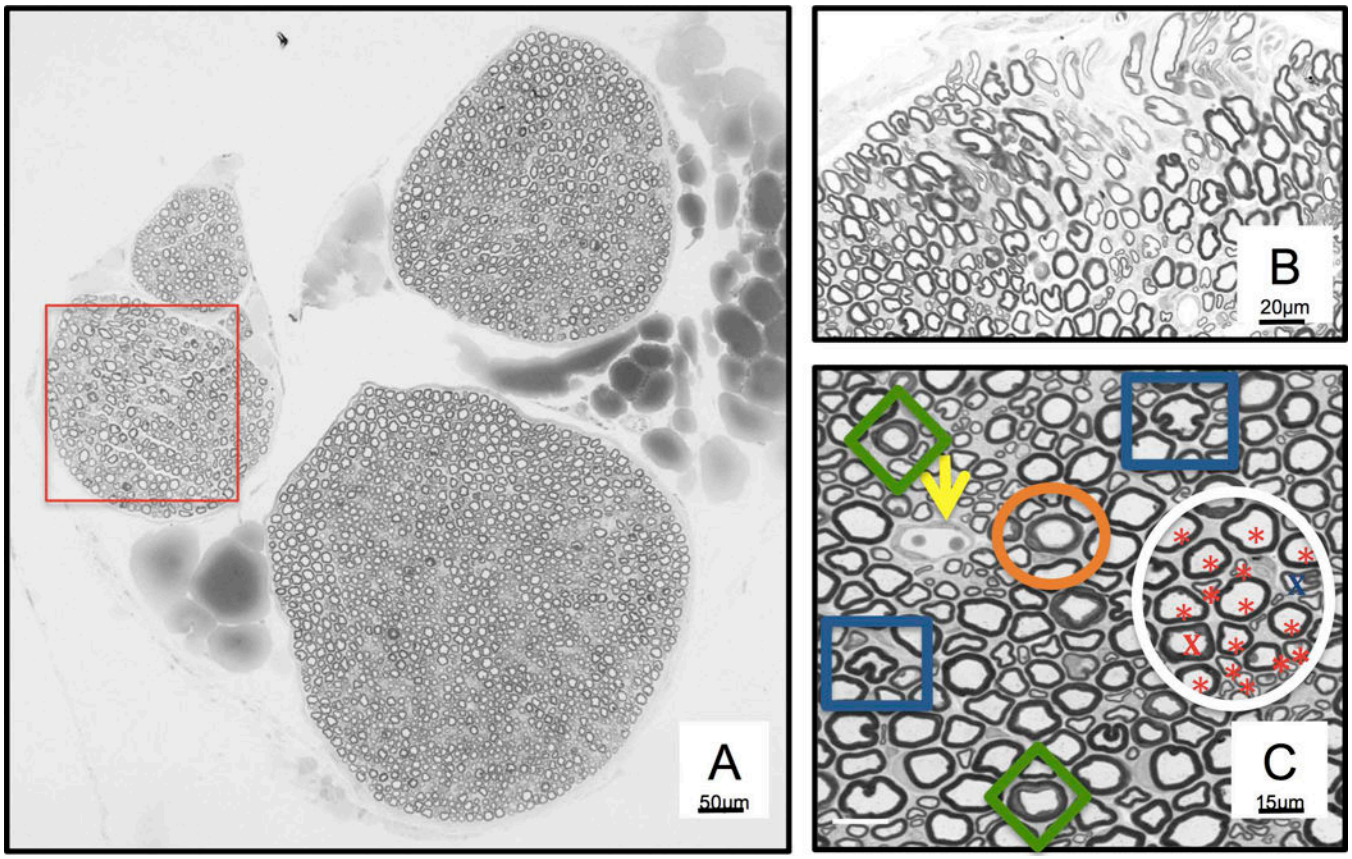

Figure 2.

A: Cross section, cut at 6 µm thickness, of a resin-fixed mouse sciatic nerve. Note the multiple fascicles embedded in fat, suggesting a distal portion of the nerve trunk and that one fascicle (red box) shows evidence of mechanical artifact. B: Mechanical damage causes distortion of axons and myelin that precludes morphometry. C: Well preserved region of nerve showing fibers viable for morphometry (examples within the white circle are indicated by a red *) and also fibers that are not quantified due to being paranodal sections (blue box and blue X), containing Schmidt-Lanterman incisures (green diamond and red X) or having a Schwann cell nucleus present (orange circle). The yellow arrow points to an endoneurial blood vessel.

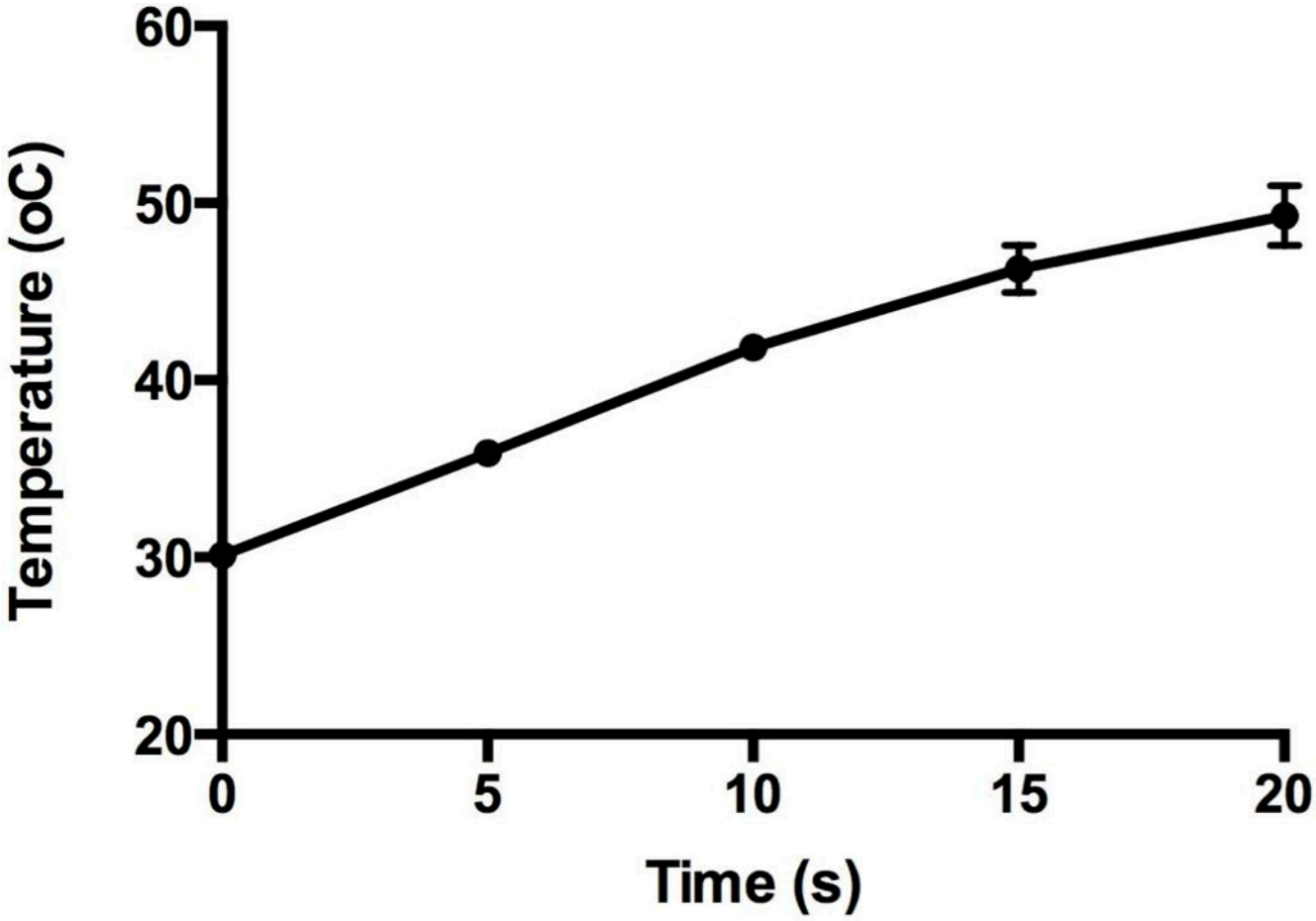

Figure 3.

Hargreaves apparatus calibration curve. Mean±sem of N=6 individual curves combined to give a daily average used to convert response time to response temperature.

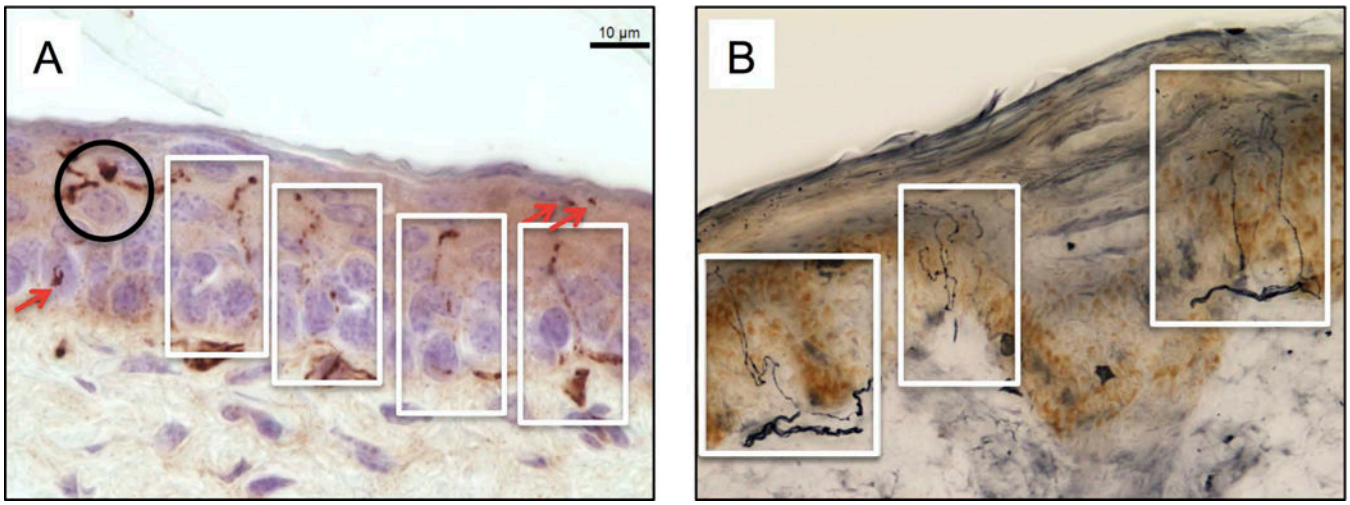

Figure 4.

A: Image of mouse skin processed in paraffin, cut at 6µm, and stained with PGP9.5. The white boxes enclose IENF that would be counted as crossing the dermal:epidermal junction (although the entire axon is only visible upon adjusting the fine focus of the microscope). Note the punctate PGP9.5 staining. The red arrows point to additional profiles included using the fragment counting method. The black circle encloses a presumptive Langerhans cell and its processes, which exhibit more intense and uniform staining that IENF. B: Image of skin processed as a frozen section, cut at 50µm, stained with PGP9.5 and imaged using a program (Image-Pro Plus, Media Cybernetics Inc.) that stacks serial images to produce a composite that facilitates tracking of individual SNP and IENF across planes of section. Within each white box is a progression of SNP to IENF. Bar = 10µm.

Figure 5.
Placement of a mouse on the custom designed platform for corneal imaging. The anesthesia delivery system is visible to the left of the image and the objective of the corneal confocal microscope with tomocap installed is at the center of the image.

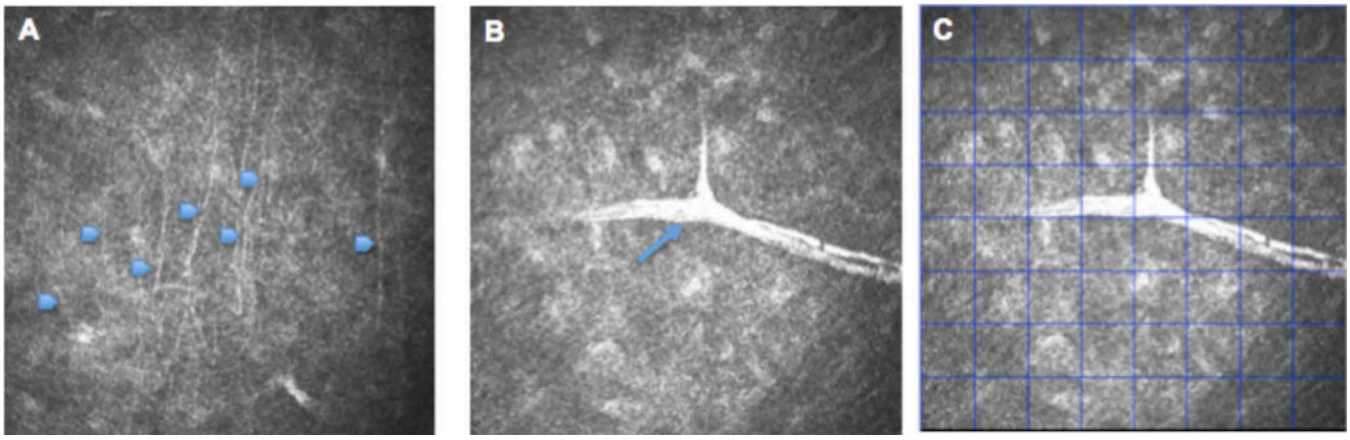

Figure 6.

Confocal images of mouse cornea. (**A**) Sub-basal nerves (arrowheads), (**B**) stromal nerve (arrow) and (**C**) stromal nerve image with a counting grid overlay that gives an occupancy score of 10/64 grids.

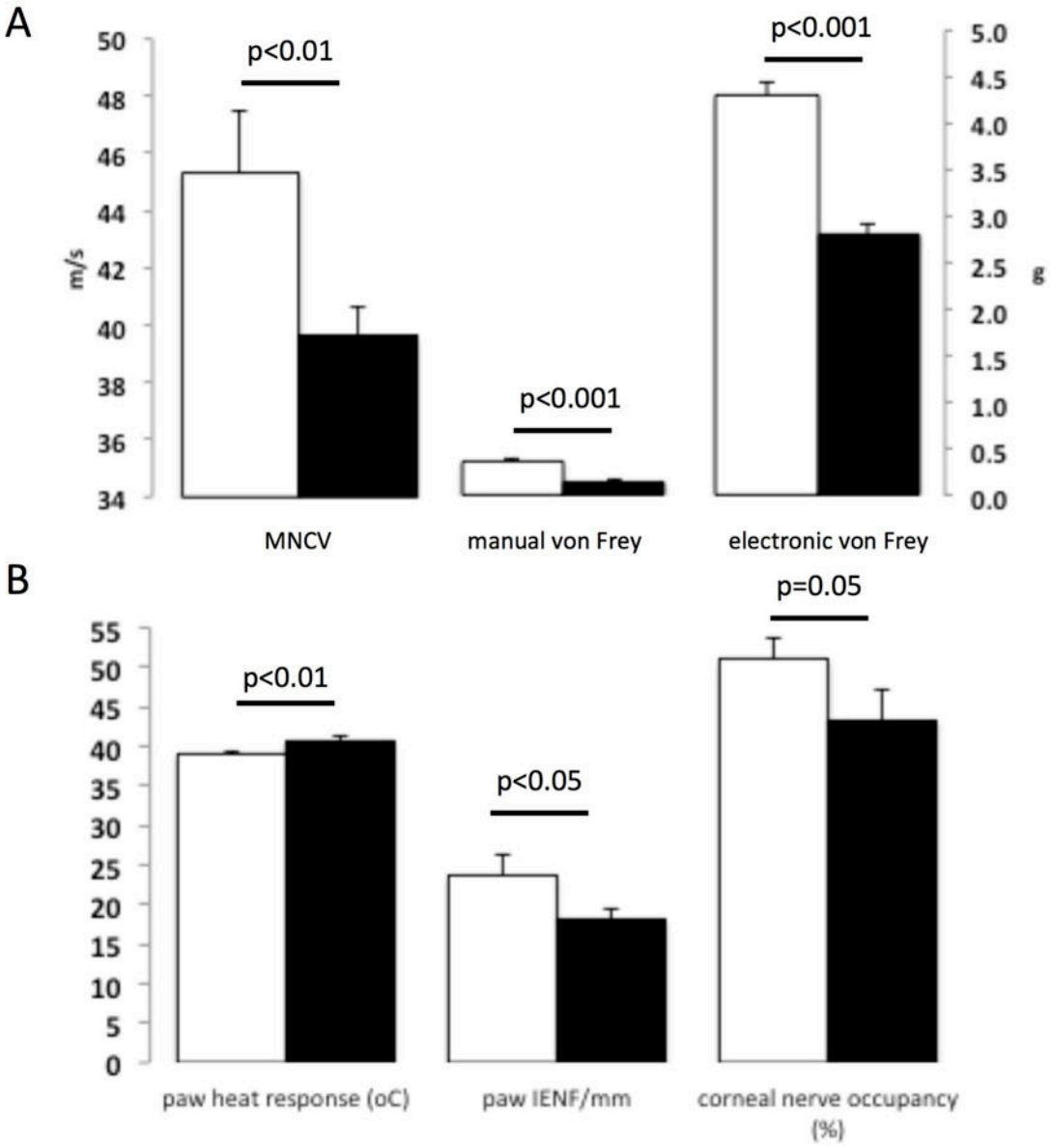

Figure 7.

Indices of large (A) and small (B) fiber neuropathy in adult female C57Bl/6J mice after 8 weeks of STZ-induced diabetes (black bars) compared to values in age-matched adult female C57Bl/6J mice (control: white bars). Data are group (N=9–10) mean ± SEM with statistical comparison by unpaired 1 tailed t test.

TABLE 1

Physiological parameters after 8 weeks of STZ-induced diabetes in adult female C57 Bl/6J mice. Data are group mean ± SEM of N= 9–10/group.

	Body weight at onset of diabetes (g)	Body weight at week 8 of diabetes (g)	Blood glucose at week 8 of diabetes (mmol/l)	Rotarod performance at week 8 of diabetes (seconds)
Control	20.1±0.3	21.6±0.5	6.8±0.3	45.3±3.7
STZ-diabetic	20.5±0.3	19.9±0.6	16.0±1.4	41.6±5.0
t test		$p<0.05$	$p<0.001$	